J|A|C|S ARTICLES

Published on Web 11/24/2010

Coordination Properties of Zinc Finger Peptides Revisited: Ligand Competition Studies Reveal Higher Affinities for Zinc and Cobalt

Olivier Sénèque* and Jean-Marc Latour*

Laboratoire de Chimie et Biologie des Métaux, CEA/iRTSV/LCBM, UMR 5249 CNRS/Université Joseph Fourier/CEA-Grenoble, 17 rue des Martyrs, 38054 Grenoble, France

Received June 8, 2010; E-mail: olivier.seneque@cea.fr; jean-marc.latour@cea.fr

Abstract: Zinc fingers are ubiquitous small protein domains which have a $Zn(Cys)_{4-x}(His)_x$ site. They possess great diversity in their structure and amino acid composition. Using a family of six peptides, it was possible to assess the influence of hydrophobic amino acids on the metal−peptide affinities and on the rates of metal association and dissociation. A model of a treble-clef zinc finger, a model of the zinc finger site of a redox-switch protein, and four variants of the classical $\beta\beta\alpha$ zinc finger were used. They differ in their coordination set, their sequence length, and their hydrophobic amino acid content. The speciation, metal binding constants, and structure of these peptides have been investigated as a function of pH. The zinc binding constants of peptides, which adopt a well-defined structure, were found to be around 10^{15} at pH 7.0. The rates of zinc exchange between EDTA and the peptides were also assessed. We evidenced that the packing of hydrophobic amino acids into a well-defined hydrophobic core can have a drastic influence on both the binding constant and the kinetics of metal exchange. Notably, well-packed hydrophobic amino acids can increase the stability constant by 4 orders of magnitude. The half-life of zinc exchange was also seen to vary significantly depending on the sequence of the zinc finger. The possible causes for this behavior are discussed. This work will help in understanding the dynamics of zinc exchange in zinc-containing proteins.

Introduction

Zinc fingers are small protein domains where a Zn^{2+} ion is bound to the protein by four cysteine or histidine side chains in tetrahedral geometry.[1] The number of cysteines varies from two to four, giving rise to $Zn(Cys)_2(His)_2$, $Zn(Cys)_3(His)$, and $Zn(Cys)_4$ sites. Zinc fingers can act as active sites, redox switches, or structural sites. Zinc fingers serving as active sites are rare, but they have been identified in enzymes such as the DNA repair protein ADA which removes methyl groups from DNA backbone phosphoesters due to a zinc-bound cysteine.[2,3] Redox-switch zinc fingers have recently been identified in proteins involved in cellular defense against oxidative stress, such as the bacterial holdase Hsp33,[4,5] the bacterial anti-σ factors RsrA[6] and ChrR,[7,8] or the mammalian Keap1 protein which regulates the antioxidant response.[9] However, most zinc fingers are pure structural sites.[1] These structural zinc finger domains have recently been classified into seven groups according to their fold with the classical $\beta\beta\alpha$, the gag knuckle, the treble-clef, and the zinc ribbon folds as the most often encountered structures.[1] These domains are rather exposed to solvent and can be constituted of mainly hydrophilic amino acids as in the heat-shock protein Hsp40[10] or may contain a hydrophobic core in the vicinity of the $Zn(Cys)_{4-x}(His)_x$ set as in classical $\beta\beta\alpha$ zinc fingers or treble-clef zinc fingers of a DNA binding domain.[1,11] A considerable amount of literature has been devoted to the identification, characterization, and biological function of zinc fingers in proteins in the past 30 years, and proteins containing a $Zn(Cys)_{4-x}(His)_x$ ($x = 1, 2, 3$) site are still regularly discovered, increasing the number of known zinc finger proteins. This number has been predicted to reach 8% of total proteins in humans by a recent bioinformatic study.[12]

Zinc fingers are generally distinct protein structure elements that only require zinc to fold correctly. For this reason, a small peptide corresponding to the sequence of zinc finger domains of a large protein can be studied independently. Most studies dealing with the metal binding properties of zinc fingers focused on the structural characterization of these domains by crystal-

(1) Krishna, S. S.; Majumdar, I.; Grishin, N. V. *Nucleic Acids Res.* **2003**, *31*, 532–550.
(2) Penner-Hahn, J. *Curr. Opin. Chem. Biol.* **2007**, *11*, 166–171.
(3) Takinowaki, H.; Matsuda, Y.; Yoshida, T.; Kobayashi, Y.; Ohkubo, T. *Protein Sci.* **2006**, *15*, 487–497.
(4) Janda, I.; Devedjiev, Y.; Derewenda, U.; Dauter, Z.; Bielnicki, J.; Cooper, D. R.; Graf, P. C. F.; Joachimiak, A.; Jakob, U.; Derewenda, Z. S. *Structure* **2004**, *12*, 1901–1907.
(5) Kumsta, C.; Jakob, U. *Biochemistry* **2009**, *48*, 4666–4676.
(6) Li, W.; Bottrill, A. R.; Bibb, M. J.; Buttner, M. J.; Paget, M. S. B.; Kleanthous, C. *J. Mol. Biol.* **2003**, *333*, 461–472.
(7) Newman, J. D.; Anthony, J. R.; Donohue, T. J. *J. Mol. Biol.* **2001**, *313*, 485–499.
(8) Campbell, E. A.; Greenwell, R.; Anthony, J. R.; Wang, S.; Lim, L.; Das, K.; Sofia, H. J.; Donohue, T. J.; Darst, S. A. *Mol. Cell* **2007**, *27*, 793–805.
(9) Dinkova-Kostova, A. T.; Holtzclaw, W. D.; Wakabayashi, N. *Biochemistry* **2005**, *44*, 6889–6899.
(10) Fan, C. Y.; Ren, H. Y.; Lee, P.; Caplan, A. J.; Cyr, D. M. *J. Biol. Chem.* **2005**, *280*, 695–702.
(11) Krizek, B. A.; Amann, B. T.; Kilfoil, V. J.; Merkle, D. L.; Berg, J. M. *J. Am. Chem. Soc.* **1991**, *113*, 4518–4523.
(12) Andreini, C.; Banci, L.; Bertini, I.; Rosato, A. *J. Proteome Res.* **2006**, *5*, 196–201.

10.1021/ja104992h

lography or NMR and on the thermodynamics of zinc binding. By contrast, the kinetics of zinc association and dissociation have scarcely been explored,[13−15] although this aspect is crucial to understand the availability and exchange process of zinc in cells.[16] The total concentration of zinc in cells is ca. 200−300 μM, but the free zinc concentration is in the picomolar to nanomolar range.[16] This implies that the concentration of zinc is finely regulated and that dynamic processes in which zinc is associated with/dissociated from proteins or is exchanged between proteins constantly take place to ensure the low free zinc concentration. The dynamic aspect of zinc−proteins interaction is crucial to understand the distribution of zinc in cells, the mechanisms of zinc transporters and sensors, and how the activity of zinc proteins can be regulated. A greater knowledge of the dynamics of zinc in cells and its origins is therefore required, which will equally aid evaluation of the potentially deleterious effects caused by stresses (oxidative, acidic, metal ions, ...) on zinc fingers and zinc proteins.

Zinc finger proteins are typically unfolded in the *apo*-state, and they acquire a defined structure when they bind Zn^{2+}. Thus, the amino acid sequence, three-dimensional structure, and thermodynamics of the metal coordination are intimately related. For example, it has been reported that deletion of a single amino acid in the ADR1 zinc finger resulted in a peptide that was unable to adopt the $\beta\beta\alpha$ fold of the native sequence.[17] Similarly, the mutations of hydrophobic residues (phenylalanine, tyrosine, and leucine) into alanine could impact the speciation and metal binding constant of a zinc finger peptide.[18] As far as thermodynamics is concerned, the affinity of various zinc finger peptides for Zn^{2+} ranges over nearly 7 orders of magnitude ($10^{8.2}$−$10^{14.7}$) at pH 7.0 and thus appears to be highly sequence dependent.[19,20] It is worth noting that the Cys_4, Cys_3His, and Cys_2His_2 variants of the nonstructured peptide GGG, composed essentially of glycines, present comparable affinities at pH 7.0.[21] This suggests that the differences in binding constants measured for other peptides might arise from differences in the second coordination sphere (hydrogen-bond network, packing of hydrophobic amino acids, etc.) rather than in the first coordination sphere. One can therefore expect a significant influence of the amino acid sequence and of the second sphere interactions in the folded form on the kinetics of association/dissociation of the metal. However, to the best of our knowledge, this has never been investigated.

We addressed this question with a set of six zinc finger peptides that have different hydrophobic amino acid contents in their sequence. We used small peptides modeling the $Zn(Cys)_4$ treble-clef zinc finger[20,22] and the $Zn(Cys)_4$ redox-switch site of Hsp33[4,23] as well as the three variants (Cys_2His_2, Cys_3His, and Cys_4) of the consensus peptide CP1, a model of the classical $\beta\beta\alpha$ zinc fingers.[11,24] Finally, the sixth peptide is another variant of CP1 lacking one amino acid in its sequence. The speciation, metal binding properties, and solution structure of these small peptides (20−26 amino acids) were carefully characterized. Herein, we show that the binding constants of the CP1 peptides are ∼3 orders of magnitude higher than that previously reported[24] with an apparent zinc binding constant of ca. 10^{15} at pH 7.0 for the Cys_2His_2 and Cys_3His variants, suggesting that classical $\beta\beta\alpha$ zinc fingers are more stable than generally believed. The Zn^{2+} complex of the CP1 variant that lacks one amino acid is 10^4 less stable than that of the full-length peptide. The difference between the two peptides is ascribed to the packing of the hydrophobic amino acids that is deficient in the shorter peptide, as shown by a structural study. We also show that the kinetics of metal exchange with EDTA can be considerably slowed down by formation of a well-packed hydrophobic core. Our work suggests that a hydrophobic core composed of a few amino acids may act as a template that controls both the thermodynamic of metal binding and the kinetics of metal exchange, even for small metallopeptides composed of ca. 25 amino acids.

Scheme 1. Zinc Finger Peptides Used in This Work

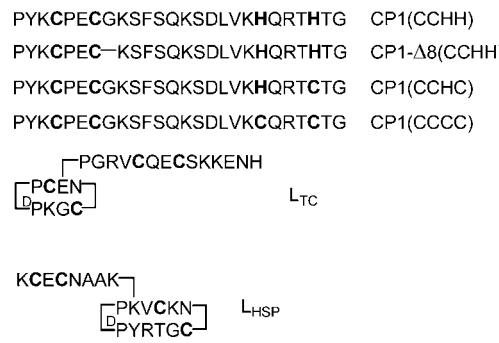

Results

Description of the Peptides. We are currently investigating the reactivity of zinc fingers with reactive oxygen species in order to get deeper insight into their involvement in oxidative stress. For that purpose, we developed structurally related models of the structural $Zn(Cys)_4$ treble-clef zinc finger[20] ($Zn\cdot L_{TC}$) and of the redox-switch $Zn(Cys)_4$ site of Hsp33 ($Zn\cdot L_{HSP}$).[23] These two models are made of a cyclic peptide that bears a linear sequence grafted on one side chain of the cycle. The cycle and linear part each incorporate a pair of cysteines. Although the size of these peptides is rather modest (22 and 20 amino acids), their zinc complexes reproduce almost perfectly the structure of the native protein sites, including the backbone folding around zinc, the orientation of the side chains, especially those of cysteines and of their hydrogen-bonded partners, and the hydrogen-bond network. Their sequence and structure are displayed in Scheme 1 and Figure 1. All hydrophobic amino acid residues in $Zn\cdot L_{TC}$ (three prolines and one valine) are exposed to solvent, unlike $Zn\cdot L_{HSP}$ which possesses a tyrosine whose aromatic ring is sandwiched between the methyl group of the threonine of the cycle and some CO and CH groups of

(13) Bombarda, E.; Grell, E.; Roques, B. P.; Mely, Y. *Biophys. J.* **2007**, *93*, 208–217.
(14) Bombarda, E.; Roques, B. P.; Mely, Y.; Grell, E. *Biochemistry* **2005**, *44*, 7315–7325.
(15) Heinz, U.; Kiefer, M.; Tholey, A.; Adolph, H. W. *J. Biol. Chem.* **2005**, *280*, 3197–3207.
(16) Maret, W.; Li, Y. *Chem. Rev.* **2009**, *109*, 4682–4707.
(17) Parraga, G.; Horvath, S.; Hood, L.; Young, E. T.; Klevit, R. E. *Proc. Natl. Acad. Sci. U.S.A.* **1990**, *87*, 137–141.
(18) Michael, S. F.; Kilfoil, V. J.; Schmidt, M. H.; Amann, B. T.; Berg, J. M. *Proc. Natl. Acad. Sci. U.S.A.* **1992**, *89*, 4796–4800.
(19) Witkiewicz-Kucharczyk, A.; Bal, W. *Toxicol. Lett.* **2006**, *162*, 29–42.
(20) Sénèque, O.; Bonnet, E.; Joumas, F. L.; Latour, J. M. *Chem.—Eur. J.* **2009**, *15*, 4798–4810.
(21) Reddi, A. R.; Guzman, T. R.; Breece, R. M.; Tiemey, D. L.; Gibney, B. R. *J. Am. Chem. Soc.* **2007**, *129*, 12815–12827.
(22) Grishin, N. V. *Nucleic Acids Res.* **2001**, *29*, 1703–1714.
(23) Sénèque, O.; Bourlès, E.; Lebrun, V.; Bonnet, E.; Dumy, P.; Latour, J. M. *Angew. Chem., Int. Ed.* **2008**, *47*, 6888–6891.
(24) Krizek, B. A.; Merkle, D. L.; Berg, J. M. *Inorg. Chem.* **1993**, *32*, 937–940.

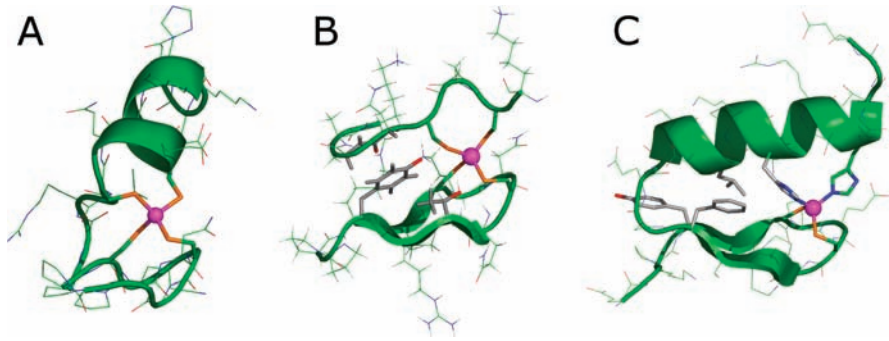

Figure 1. Structures of the zinc complexes of $Zn\cdot L_{TC}$ (A) and $Zn\cdot L_{HSP}$ (B) and structure of a classical $\beta\beta\alpha$ zinc finger (C). The hydrophobic cores of $Zn\cdot L_{HSP}$ and the classical $\beta\beta\alpha$ zinc finger are highlighted in gray. The zinc ion is shown in purple. The figure was generated using Pymol.[34]

the linear chain, thereby constituting a small hydrophobic core. In order to evaluate the role of the hydrophobic core on the coordination properties of zinc fingers, we looked for peptides with more hydrophobic amino acids. Among the various zinc finger structures, one of the most encountered is that of the classical $\beta\beta\alpha$ Cys_2His_2 zinc fingers. These fingers possess a conserved sequence of the form (Tyr/Phe)-Xaa-Cys-$Xaa_{2,4}$-Cys-Xaa_3-Phe-Xaa_5-Leu-Xaa_2-His-Xaa_{3-5}-His, where Xaa corresponds to any amino acid. They adopt the $\beta\beta\alpha$ fold displayed in Figure 1. The three conserved hydrophobic amino acids (Tyr or Phe, Phe and Leu) and one of the two histidines form an extended hydrophobic core between the β-hairpin and the helix. In pioneering work on designed metallopeptides, Berg et al. described at the beginning of the 1990s the CP1(CCHH) peptide which corresponds to the consensus sequence of such fingers.[11] The Zn·CP1(CCHH) complex behaves as all classical $\beta\beta\alpha$ zinc fingers and has been used by Berg and others as a prototype of these zinc fingers[11,25,26] but also as a tool to measure the binding constants of zinc proteins[27−29] or to quantify interactions between amino acids found in proteins.[30−32] The Cys_3His and Cys_4 variants of CP1(CCHH), namely, CP1(CCHC) and CP1(CCCC) (Scheme 1), were also used to examine the influence of the coordination set on the metal binding properties, but less attention was paid to their structural characterization.[24] Recently, Heinz et al. used a shorter version of this peptide, CP1-Δ8(CCHH), to investigate the kinetics of metal exchange of zinc finger peptides with EDTA.[15] This peptide shares the same sequence with CP1(CCHH) but lacks the Gly in position 8, thereby changing the number of amino acids in the spacer region between the pair of cysteines and the pair of histidines. The influence of such a deletion in the spacer region, which could impact the proper folding of the peptide and formation of the hydrophobic core, has been a matter of debate. Parraga et al. found that this deletion in the ADR1 zinc finger drastically alters both the structure of the *holo*-peptide and the metal binding properties, abolishing the Co^{2+} binding and reducing the affinity for Zn^{2+}.[17] Shi et al. showed by comparing the binding constants of ADR1 and CP1(CCHH) with those of their deletion mutants that the Co^{2+} binding constants was reduced at most by 2 orders of magnitude in the deletion mutant.[33] It was stated in the same article that Zn·CP1-Δ8(CCHH) was at least partially folded, but the structural investigation was limited to examination of a 1D ^1H NMR spectrum in D_2O,[33] as was the study of Parraga et al. on the ADR1 deletion mutant.[17] Therefore, the structural features of the deletion mutants are still to be investigated. In the course of our work, we observed that EDTA only slightly displaces Zn^{2+} from Zn·CP1(CCHH), although the binding constant reported for this peptide at pH 7.0 is $10^{11.6}$, well below that of EDTA ($10^{13.1}$),[24] suggesting that the binding constants of CP1 could have been underestimated. We also observed that it took hours for equilibration to occur when EDTA was mixed to Zn·CP1(CCHH), in contrast to the equilibrium time on the order of seconds reported for Zn·CP1-Δ8(CCHH). This prompted us to fully reinvestigate the coordination properties of the four peptides of the CP1 family from thermodynamic, kinetic, and structural points of view and to compare them to L_{TC} and L_{HSP}, which have different hydrophobic amino acids contents in their sequence.

Peptide Synthesis. Berg et al. described the synthesis of CP1(CCHH) by solid-phase peptide synthesis using pentafluorophenol (OPfp) ester activation.[11] Since OPfp esters of N-α-Fmoc amino acids are expensive, we turned to the more classical PyBOP activation protocol. With polystyrene-based resin (2-chlorotritylchloride, Rink amide, or Sieber amide resin) the synthesis did not reach completion because of peptide aggregation. The situation was improved by using the poly(ethylene glycol)-based NovaPEG Rink amide resin, but a mixture of four peptides that had to be separated was obtained at the end of the synthesis. However, CP1(CCHH) and the shorter peptide lacking the N-ter PYKC motif could not be separated by HPLC. Therefore, we used the pseudoproline dipeptide Fmoc-Phe-Ser($\psi^{Me,Me}$pro)-OH to graft the Phe-Ser motif in the middle of the sequence and to prevent the peptide chain from aggregating on the resin. This yielded a crude product containing CP1(CCHH) as a major product (>95%), which was purified by HPLC and identified by ESI-MS. All the variants of the CP1 family (CP1(CCHH), CP1-Δ8(CCHH), CP1(CCHC), and CP1(CCCC)) were obtained as pure powders at the 250 mg scale. L_{TC} and L_{HSP} were synthesized as previously described.[20,23]

pK_a of the *apo*-Peptides. The pK_a of the histidine and cysteine side chains of the *apo*-peptides were measured by ^1H NMR as

(25) Clark-Baldwin, K.; Tierney, D. L.; Govindaswamy, N.; Gruff, E. S.; Kim, C.; Berg, J.; Koch, S. A.; Penner-Hahn, J. E. *J. Am. Chem. Soc.* **1998**, *120*, 8401–8409.
(26) Franzman, M. A.; Barrios, A. M. *Inorg. Chem.* **2008**, *47*, 3928–3930.
(27) Ghering, A. B.; Jenkins, L. M. M.; Schenck, B. L.; Deo, S.; Mayer, R. A.; Pikaart, M. J.; Omichinski, J. G.; Godwin, H. A. *J. Am. Chem. Soc.* **2005**, *127*, 3751–3759.
(28) Ghering, A. B.; Shokes, J. E.; Scott, R. A.; Omichinski, J. G.; Godwin, H. A. *Biochemistry* **2004**, *43*, 8346–8355.
(29) Payne, J. C.; ter Horst, M. A.; Godwin, H. A. *J. Am. Chem. Soc.* **1999**, *121*, 6850–6855.
(30) Blasie, C. A.; Berg, J. M. *Biochemistry* **1997**, *36*, 6218–6222.
(31) Blasie, C. A.; Berg, J. M. *Biochemistry* **2004**, *43*, 10600–10604.
(32) Kim, C. W. A.; Berg, J. M. *Nature* **1993**, *362*, 267–270.
(33) Shi, Y. G.; Beger, R. D.; Berg, J. M. *Biophys. J.* **1993**, *64*, 749–753.
(34) Delano, W. L. *The PyMOL Molecular Graphics System*; Delano Scientific: Palo Alto, CA, 2002.

Table 1. pK_a (298 K, $I = 0.1$ M) of the Histidine and Cysteine Side Chains Determined by ^{1}H NMR

peptide	pK_a			
CP1(CCHH)	6.3 (H)	6.3 (H)	7.7 (C)	8.7 (C)
CP1(CCHC)	6.4 (H)	7.6 (C)	8.5 (C)	8.7 (C)
CP1(CCCC)	7.6 (C)	8.1 (C)	8.7 (C)	9.1 (C)
CP1-Δ8(CCHH)	6.3 (H)	6.3 (H)	7.8 (C)	8.6 (C)
L_{HSP}	7.2 (C)	7.3 (C)	8.6 (C)	9.0 (C)
L_{TC}[a]	6.5 (C)	7.9 (C)	9.0 (C)	9.8 (C)

[a] See ref 20.

reported previously for L_{TC}.[20] The four pK_a values of the cysteine and histidine side chains of L_{HSP} and of the CP1 peptides are given in Table 1. pK_a values of histidine side chains are close to the pK_a of histidine in solution (6.5). The pK_a values of the cysteines spread over the 6.5−9.8 range, which is ca. 2 units around the pK_a of cysteine (8.3). The cysteine side chains of the CPEC motif of the four CP1 peptides have pK_a at 7.7 and 8.7 within 0.1 pH unit (estimated error of measurement).

UV and CD Characterization of Zn^{2+} and Co^{2+} Complexes. Zn^{2+} with its fully occupied d shell is a spectroscopically silent metal ion. Due to some similarity in their coordination properties, Co^{2+} often serves as a spectroscopic probe to assess the zinc binding environment in proteins. Co^{2+} has also often been used to determine the zinc binding constants of a peptide or a protein. The Co^{2+} binding constant is derived from direct titrations by monitoring the increase of the d−d transitions in the visible, and back-titration with Zn^{2+} leads to disappearance of the d−d transitions and gives the Zn^{2+} binding constant. In recent articles,[20,23] we have shown that CysS → Zn LMCT bands can be monitored in the UV region for $Zn(Cys)_4$ sites and that CD spectroscopy is a valuable tool to monitor metal binding to small peptides. The changes in the CD signal upon zinc binding reflect both the change in the structure of the peptide and the appearance of LMCT bands. Whereas the absorption spectra of the Co^{2+} complexes of CP1 peptides have systematically been reported in the literature,[24,33] the absorption spectra of the Zn^{2+} complexes and the CD spectra of the Zn^{2+} and Co^{2+} complexes were only reported in few instances.[32,35] Therefore, we reinvestigated the spectroscopic properties of Zn^{2+} and Co^{2+} complexes of all the CP1 peptides. Characterization of Zn^{2+} and Co^{2+} complexes of L_{TC} and L_{HSP} has been reported previously.[20,23] Both peptides form 1:1 metal/peptide complexes only.

Co^{2+} binding by the CP1 peptides was monitored by UV−vis and CD titrations at pH 7.0 in BisTris and phosphate buffer, respectively. For all full-length CP1 peptides (CP1(CCHH), CP1(CCHC), and CP1(CCCC)), these titrations showed formation of 1:1 cobalt/peptide complexes only (Figure 2 and Figure S1 of Supporting Information). The absorption spectra were identical to those reported by Krizek et al.[24] and correspond to pseudotetrahedral Co^{2+} complexes. The end point of the titration is very sharp. As previously reported,[33] the UV−vis titration of CP1-Δ8(CCHH) by Co^{2+} reveals formation of both 1:2 and 1:1 metal to peptide complexes, the former being formed at low metal/peptide ratio. The spectrum of the 1:1 complex resembles that of Co·CP1(CCHH), whereas the 1:2 complex shows an absorption around 720 nm which suggests that the Co^{2+} is bound by a $(Cys)_4$ or a $(Cys)_3His$ donor set.[18,33] The CD spectra of the *apo*-CP1 peptides and of their Co^{2+} complexes

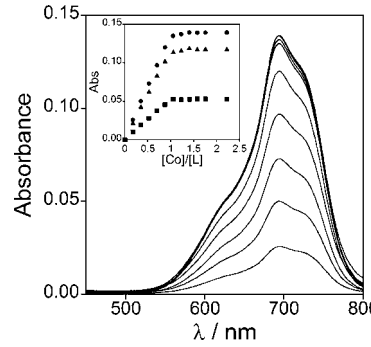

Figure 2. UV−vis titration of CP1(CCCC) 179 μM by Co^{2+} in BisTris 100 mM/KCl, 100 mM, pH 7.0, TCEP 270 μM, 298 K (path length 1 cm). Spectra were corrected for dilution. The inset shows the evolution of the d−d transitions at 630 (squares), 693 (circles), and 725 nm (triangles) against the Co^{2+}/peptide ratio.

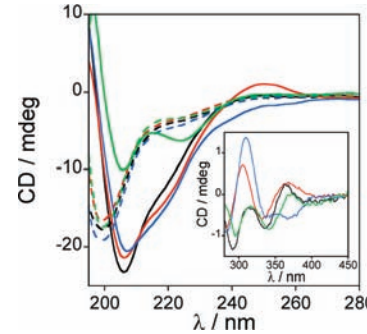

Figure 3. CD spectra of the *apo*-CP1 peptides (dashed lines) and Co·CP1 complexes (solid lines). CP1(CCHH), black; CP1(CCHC), red; CP1(CCCC), blue; CP1-Δ8(CCHH), green. [CP1] = 17 μM in phosphate buffer 20 mM pH 7.0, TCEP 250 μM, 298 K (path length 0.4 cm). (Inset) CD spectra of the Co·CP1 in the 280−450 nm region.

are displayed in Figure 3. The CD signatures of the four CP1 *apo*-peptides are characteristic of a random coil conformation. For all three full-length CP1 peptides, addition of 1 mol equiv of Co^{2+} leads to an increase of the negative CD signal above 205 nm and a more positive signal below 205 nm. The positive and negative bands observed in the 280−400 nm region are contributions of the CysS → Co LMCT absorptions to the CD signal. These LMCT contributions preclude a direct analysis of the structural changes caused by metal binding. The CD spectrum of Co·CP1-Δ8(CCHH) obtained with excess Co^{2+} differs significantly from that of Co·CP1(CCHH). These differences can arise either from different folding or from different signatures of the LMCT bands.

Zinc titrations in phosphate buffer were monitored by UV−vis spectroscopy. For each of the four CP1 peptides, a band appears around 220 nm with increasing amounts of Zn^{2+} until a plateau is reached at 1.0 equiv of zinc ion (Figure 4) with a sharp end point. This band is attributed to a CysS → Zn LMCT transition. The intensity depends on the number of cysteines in the peptide: $\Delta\epsilon_{220}$ = 8700, 6500, 15 500, and 22 300 M^{-1} cm^{-1} for Zn·CP1(CCHH), Zn·CP1-Δ8(CCHH), Zn·CP1(CCHC), and Zn·CP1(CCCC), respectively. Thus, replacement of a histidine by a cysteine in the coordination sphere of Zn^{2+} does not significantly affect the maximum of the LMCT band but increases its absorption coefficient by ∼7000 M^{-1} cm^{-1}. The evolution of the CD signal and the isodichroic point (at 205 nm for full-length CP1 and 212 nm for CP1-Δ8) confirm formation of 1:1 Zn/CP1 complexes only, even for CP-Δ8(CCHH). All Zn·CP1 complexes have different spectra but

(35) Bianchi, E.; Folgori, A.; Wallace, A.; Nicotra, M.; Acali, S.; Phalipon, A.; Barbato, G.; Bazzo, R.; Cortese, R.; Felici, F.; Pessi, A. *J. Mol. Biol.* **1995**, *247*, 154–160.

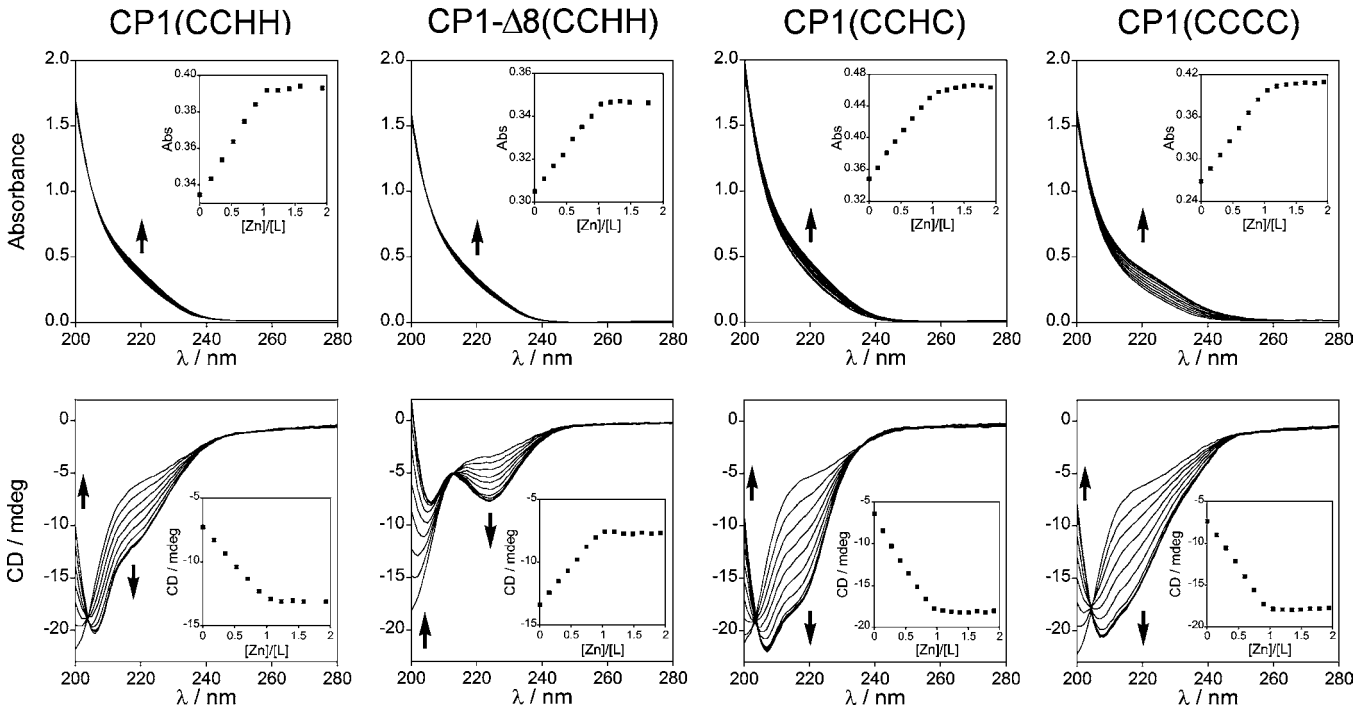

Figure 4. UV (top) and CD (bottom) titrations of CP1(CCHH) 17 μM, CP1-Δ8(CCHH) 16.5 μM, CP1(CCHC) 18.5 μM, and CP1(CCCC) 16 μM with Zn^{2+} in phosphate buffer 20 mM pH 7.0, TCEP 250 μM, 298 K (path length = 0.4 cm). (Insets) Evolution of the UV or CD signals at 220 nm for all titrations except the CD titration of CP1-Δ8(CCHH) for which the signal at 205 nm is shown.

Scheme 2. Protonation and M^{2+} Complexation Equilibria for Peptides L[a]

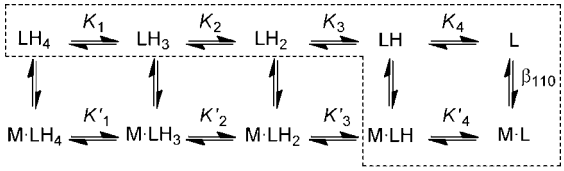

[a] The dashed box highlights the minimal set of species used to fit the variation of K_{app} against pH. K_i and K'_i correspond to the successive proton dissociation constants of the *apo*- and *holo*-peptides, respectively. β_{110} is the metal binding equilibrium constant between the fully deprotonated *apo*- and *holo*-peptides, $\beta_{110} = [ML]/[M][L]$.

with a marked difference between Zn·CP1(CCHH) and Zn·CP1-Δ8(CCHH), as already observed for the Co^{2+} complexes. It is worth noting that a 1.8-, 2.2-, 2.9-, and 2.4-fold increase of the intensity of the negative CD signal at 220 nm is observed for CP1(CCHH), CP1-Δ8(CCHH), CP1(CCHC), and CP1(CCCC), respectively, upon zinc binding. This makes CD a valuable tool to monitor zinc binding to the four peptides and to measure the zinc binding constants by competition experiments (vide infra).

pH Dependence of the Metal Binding Constants. The chemical speciation of the peptide is governed by the competition between the metal and the protons for binding the cysteine and histidine side chains. The binding of a metal ion to a peptide bearing a $(Cys)_{4-x}(His)_x$ coordination set can be described according to Scheme 2, taking into account only the protonation of the metal binding residues. Both *apo*- and *holo*-peptides may have five different protonation states (LH_i and $Zn·LH_i$, $i = 0-4$) depending on the protonation state of the cysteine and histidine side chains.

The apparent metal binding constant, K_{app}, at a given pH is defined by eq 1.

$$K_{app} = \frac{[ML]_{total}}{[M] \times [L]_{total}} = \frac{\sum_i [MLH_i]}{[M] \times (\sum_i [LH_i])} \quad (1)$$

The pH dependence of the zinc binding constant K_{app} was investigated over the pH range 4−8 for L_{HSP} and the four CP1 peptides as previously reported for L_{TC}.[20] Titrations were performed by monitoring the CD signal upon progressive addition of Zn^{2+} to a solution containing the peptide and a competitor (NTA, HEDTA, EDTA, TPEN) whose apparent binding constant is known. At a given pH, the competitor was chosen so that its K_{app} matches that of the peptide within 2 orders of magnitude. Fitting the titrations yielded the ratio of K_{app}(peptide)/K_{app}(competitor) and thus the K_{app} for the peptide. Representative examples of these titrations are provided in the Supporting Information. The time needed to reach the equilibrium depended on both the peptide and the pH and could be up to several hours (vide infra). For the lowest pH where K_{app} is below 10^6, direct titrations (without competitor) were performed. The values of log(K_{app}) for zinc are plotted against pH in Figure 5 for all the peptides studied here. A strong pH dependence of K_{app} is observed, and the slope of the increase of log(K_{app}) in the linear part (between pH 5.0 and 6.5) is 3.4−3.9 per pH unit, in excellent agreement with the binding of the four cysteines or histidines to zinc. Whereas CP1(CCHH) and CP1(CCHC) peptides have similar K_{app} below pH 7.5, the four cysteines variant CP1(CCCC) has K_{app} values about 2.5 orders of magnitude lower. The K_{app} value for Zn·CP1-Δ8(CCHH) ($K_{app} = 10^{10.6}$) that we measured at pH 7.0 by competition with HEDTA is identical to the value measured by Heinz by competition with Quin-2 at the same pH.[15] Noteworthy, deletion of Gly^8 in the sequence of CP1(CCHH) reduces the zinc binding constant by a factor of 2.5×10^4.

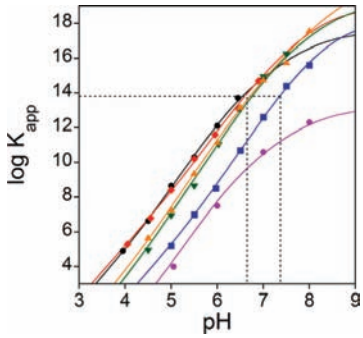

Figure 5. Plot of the measured binding constant K_{app} against pH for Zn·CP1(CCHH) (black circles), Zn·CP1(CCHC) (red diamonds), Zn·CP1(CCCC) (blue squares), Zn·CP1-Δ8(CCHH) (purple circles), Zn·L_{HSP} (green downward triangles), and Zn·L_{TC} (orange upward triangles). The solid lines correspond to fits to eq 2 with β_{110} and K'_4 values reported in Table 2. The data for Zn·L_{TC} were published previously.[20] The dashed lines identify the pH and K_{app} values chosen to compare the kinetics of zinc exchange with EDTA.

Table 2. Thermodynamic Parameters of the pH Dependence of the Zn^{2+} and Co^{2+} Binding Constants K_{app} at 298 K

	Zn^{2+} complexes			Co^{2+} complexes	
peptide	log β_{110}	pK'_4	log K_{app} at pH 7.0	log β_{110}[a]	log K_{app} at pH 7.0
CP1(CCHH)	17.5 (1)	4.5 (1)	14.9 (1)	13.2 (1)	10.6 (1)
CP1(CCHC)	18.9 (1)	5.3 (1)	15.0 (1)	nd[d]	11.0 (3)
CP1(CCCC)	18.1 (1)	5.6 (1)	12.6 (1)	14.3 (1)	8.8 (1)
CP1-Δ8(CCHH)	13.1 (1)	4.6 (2)	10.6 (1)	nd	5.8 (1)
L_{HSP}	19.2 (1)	4.1 (1)	14.6 (1)	nd	9.9 (2)[c]
L_{TC}	20.6 (1)[b]	<4.2[b]	14.7 (1)[b]	nd	11.2 (2)[b]

[a] Values of log β_{110} are given only when K_{app} was measured at different pH. [b] Values from ref 20. [c] Values from ref 23. [d] Not determined.

The apparent binding constant K_{app} can be expressed as a function of pH according to Scheme 2. Equation 2 describes the evolution of K_{app} as the pH varies and can be used to fit the experimental data. Its derivation is given in the Supporting Information. In order to avoid overparameterization of the system, we searched for the minimal set of species that could fit the pH dependence of K_{app}. First, only the fully deprotonated complex Zn·L was introduced in the fit in addition to the five protonation states of the *apo*-peptide, and thus, the only parameter to refine was β_{110}. The fits were excellent above pH 5.0 for CP1(CCHH) and CP1(CCHC) and above pH 6.0 for CP1(CCCC), yielding reliable values for β_{110} (values in Table 2), but it was necessary to introduce the Zn·LH complex and thus K'_4 as a second parameter to fully reproduce the experimental data below pH 5.0. The fits to eq 2 corresponding to the set of species in the dashed box in Scheme 2 are displayed in Figure 5. The pK'_4 values were 4.4, 5.3, and 5.5 for CP1(CCHH), CP1(CCHC), and CP1(CCCC), respectively. For CP1-Δ8(CCHH), the experimental data could be fitted with a value of $10^{13.1}$ for β_{110} and any pK'_4 below 4.6, indicating that the monoprotonated complex Zn·LH is not formed in a significant amount at pH values above 5.0 where the K_{app} was measured.

$$K_{app} = \beta_{110}\frac{1 + 10^{(pK'_4 - pH)}}{1 + 10^{(pK_4 - pH)} + 10^{(pK_3 + pK_4 - 2pH)} + 10^{(pK_2 + pK_3 + pK_4 - 3pH)} + 10^{(pK_1 + pK_2 + pK_3 + pK_4 - 4pH)}} \quad (2)$$

To confirm these results, pH titrations of the Zn·CP1 complexes were performed and monitored by CD spectroscopy. The data were fitted using SPECFIT/32[36] with the five protonation states of the *apo*-peptide LH_i ($i = 0-4$) and the Zn·L complex only. The proton dissociation constants of the *apo*-peptide (K_i) measured by NMR and the β_{110} determined from the pH dependence of K_{app} were fixed. However, the results were not satisfactory. For each of the four CP1 peptides, it was necessary to introduce the Zn·LH complex to correctly reproduce the experimental data (Figure 6). The pK'_4 values obtained (4.5 (1), 5.3 (1), 5.7 (1), and 4.6 (2) for CP1(CCHH), CP1(CCHC), CP1(CCCC), and CP1-Δ8(CCHH), respectively) match perfectly those obtained from the fit of the pH dependence of K_{app}.

For L_{HSP}, the pH dependence of K_{app} could be satisfactorily fitted on the whole pH range by introducing Zn·L_{HSP} as the sole complex form ($\beta_{110} = 10^{19.2}$). This indicates that Zn·L_{HSP}H is not formed in a significant amount even in the lower pH explored and that K'_4, the pK_a of the Zn·L_{HSP}H/Zn·L_{HSP} couple, is below 4.5. However, Zn·L_{HSP}H was needed to correctly reproduce the data of the pH titration monitored by CD (Figure 6) with a pK'_4 value of 4.2 (1). This value, which is similar to that measured for L_{TC}, is ca. 1.5 units lower than that of CP1(CCCC), showing that Zn·CP1(CCCC) is more prone to protonation than the two other $Zn(Cys)_4$ complexes. The species distribution against pH is given in Figure 6. For the full-length CP1 peptides, there is a pH domain below pH 6.0 where the monoprotonated complex Zn·LH is the predominant species. However, at pH 7.0, the fully deprotonated form of the complex is always the major form with Zn·LH never exceeding 1% except for CP1(CCCC) for which 5% of the complex is in the monoprotonated form.

The apparent Co^{2+} binding constants of the CP1 peptides were assessed at pH 7.0. For CP1(CCCC), K_{app} was derived from a titration of the Co·CP1(CCCC) complex by Zn^{2+}, in conditions of excess Co^{2+} (see Figure S5 of Supporting Information). For CP1(CCHH) and CP1(CCHC), cobalt binding competition experiments between CP1 and HEDTA were performed. The values of K_{app} at pH 7.0 for Co^{2+} are summarized in Table 2. The value at pH 7.0 obtained for CP1(CCHH) was confirmed by direct titrations at lower pH (5.0 and 5.5). These values match perfectly the expected pH dependence of K_{app} with log β_{110} = 13.2 (1) (see the plot of log K_{app} against pH in Figure S6 of Supporting Information). For CP1-Δ8(CCHH), the apparent binding constants of the 1:1 and 1:2 Co^{2+}/peptide complexes at pH 7.0 were derived from the fit of the variation of the absorption spectrum during a direct titration experiment. The fit was performed with SPECFIT/32, taking into account the known binding constant of the buffer (BisTris) for Co^{2+}.[29,37] The logarithms of the apparent formation constant of the 1:1 and 1:2 Co^{2+} complexes of CP1-Δ8(CCHH) were, respectively, 5.8 (1) and 8.9 (4). As expected from the direct titrations, all three full-length CP1 peptides form tight complexes with Co^{2+} with K_{app} values above 10^7, but the affinity of CP1-Δ8(CCHH) is considerably reduced in comparison with CP1(CCHH): K_{app}(Co·CP1(CCHH))/K_{app}(Co·CP1-Δ8(CCHH)) = 6.3×10^4.

Structural Characterization of the Zn·CP1 Complexes. Natural CCHC zinc fingers that adopt a $\beta\beta\alpha$ fold have been characterized.[38] They have a sequence similar to that of CP1(CCHC)

(36) Binstead, R.; Zuberbühler, A. *SPECFIT Global Analysis System*, Version 3.0; Spectrum Software Associates: Marlborough, MA, 2000.
(37) Scheller, K. H.; Abel, T. H. J.; Polanyi, P. E.; Wenk, P. K.; Fischer, B. E.; Sigel, H. *Eur. J. Biochem.* **1980**, *107*, 455–466.
(38) Liew, C. K.; Kowalski, K.; Fox, A. H.; Newton, A.; Sharpe, B. K.; Crossley, M.; Mackay, J. P. *Structure* **2000**, *8*, 1157–1166.

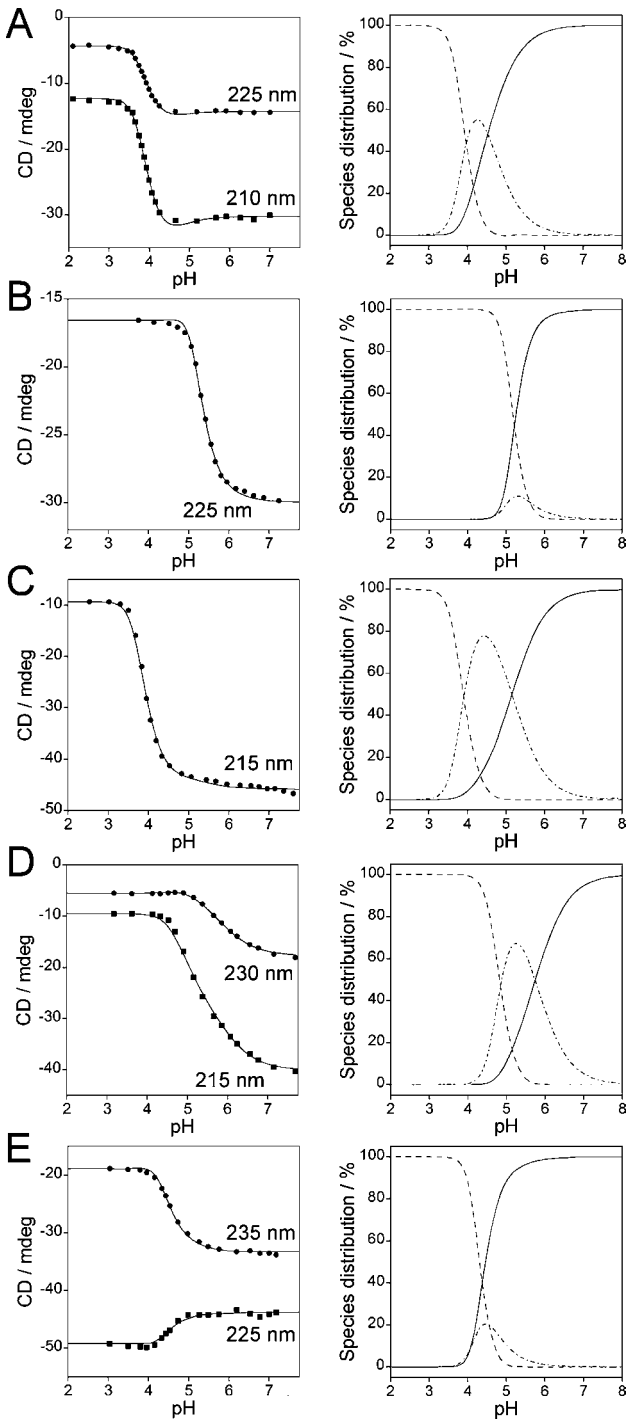

Figure 6. pH titrations of Zn·CP1(CCHH) (A), Zn·CP1-Δ8(CCHH) (B), Zn·CP1(CCHC) (C), Zn·CP1(CCCC) (D), and Zn·L_{HSP} (E) monitored by CD spectroscopy. (Left) Variation of the CD signal against pH. The solid line corresponds to the fit obtained with SPECFIT/32. (Right) Species distribution of Zn·L (solid line), Zn·LH (dashed and dotted line), and the *apo*-peptide (dashed line). The titrations were performed with 1.1 equiv of Zn^{2+}/peptide, and the peptide concentrations were 19.5, 25, 23, 18.5, and 60 μM for CP1(CCHH), CP1-Δ8(CCHH), CP1(CCHC), CP1(CCCC), and L_{HSP}, respectively.

with only an additional amino acid between the histidine and the C-terminal cysteine ($FX_2CX_{2,4}CX_3FX_5LX_2HX_4C$). Therefore, the structure of Zn·CP1(CCHC) is anticipated to resemble that of Zn·CP1(CCHH). However, this $\beta\beta\alpha$ fold is not common for CCCC zinc fingers, which mostly adopt treble-clef or zinc-ribbon folds.[1] It has thus to be checked if Zn·CP1(CCCC) can adopt this fold. The solution structure of the zinc complexes of CP1(CCHC) and CP1(CCCC) complexes were investigated by ^{1}H NMR in order to compare their folding with that of Zn·CP1(CCHH). TOCSY, COSY, and NOESY spectra were recorded for Zn·CP1(CCHH) and Zn·CP1(CCHC) at pH 6.5 where 99% and 96%, respectively, of the complex is in the fully deprotonated form ZnL. The assignments of the protons are given in the Supporting Information (Tables S1−S6). Table 3 gives selected chemical shifts that are typical of the solution structure of Zn·CP1(CCHH).[39] Figure 7 shows the chemical shift index (CSI) of the Hα protons of the Zn·CP1 complexes, and Figure S8 of Supporting Information compares the chemical shifts of Hα protons of Zn·CP1(CCHH) with those of a random coil peptide. The ^{1}H NMR spectra of Zn·CP1(CCHH) and Zn·CP1(CCHC) are well defined with sharp peaks except for the NH resonances of Ser^{12} and Lys^{14} which are too broad to be located, as previously observed.[39] The comparison of the data obtained for Zn·CP1(CCHC) and Zn·CP1(CCHH) shows that they adopt the same overall $\beta\beta\alpha$ fold. The broad NH resonances in the $S^{12}QK^{14}$ motif suggest some flexibility in the loop between the β-hairpin and the helix. The major differences in the chemical shifts are observed for the four C-ter amino acids, where the His to Cys mutation was introduced. The Hα CSI of Zn·CP1(CCHC) suggests that the C-ter helix extends from Lys^{14} to Arg^{22} and is thus one amino acid shorter than in Zn·CP1(CCHH). In addition, the $^3J_{NH,H\alpha}$ of Thr^{23} in Zn·CP1(CCHH) is 10.4 Hz, which shows that this residue does not belong to the helix. The cysteine introduced in place of His^{24} has a shorter side chain. In order to bind the cysteine sulfur to zinc, the C-ter of the peptide has to adopt a different conformation. Finally, the key chemical shifts given in Table 3 and the NOE pattern involving the side chains of the hydrophobic amino acids ($Phe^{11}H\delta,\epsilon$/$Leu^{17}H\alpha$, $Ser^{10}H\alpha$/$Phe^{11}H\delta,\epsilon$, Cys^4HN/$Phe^{11}\delta,\epsilon$, $Tyr^2H\epsilon$/$Lys^{14}H\beta,\gamma$, and $Phe^{11}H\zeta$/$His^{20}H\delta,\epsilon$) are similar for Zn·CP1(CCHC) and Zn·CP1(CCHH). This fully agrees with the same packing of the hydrophobic core in the two complexes.

For the zinc complex of CP1(CCCC), the spectra were recorded at pH 5.1, 6.5, and 7.1. At these pH values, the proportions of Zn·L and Zn·LH are 24:76, 89:11, and 98:2, respectively, and the *apo*-peptide is not present. Whatever the pH, only one set of signals is observed, thereby indicating that Zn·L and Zn·LH forms are in fast exchange on the NMR time scale. The chemical shifts at pH 6.5 and 7.1 are almost identical but with broader NH resonances at pH 7.1 because of exchange with water. Therefore, only the data at pH 6.5 will be discussed. At pH 6.5, the NH resonances of the N-ter $V^{18}KCQRTC^{24}$ motif are broader than the others but all of them could be assigned. The chemical shifts are similar to those of Zn·CP1(CCHH). Hα CSI show, however, that the helix is shorter than in the CCHH and CCHC variants and extends from Lys^{14} to Cys^{20}. Table 3 highlights that all the key chemical shifts remain in the same range, except Phe^{11} Hζ, which is close to the random coil value. In the structure of Zn·CP1(CCHH), this proton faces the aromatic ring of His^{20}. Hence, its high-field shift in Zn·CP1(CCHH) is due to the imidazole ring currents. As this histidine is mutated into a cysteine in the CCCC variant, such an effect cannot be observed. In addition to the conservation of these key chemical shifts, the same set of NOE that is observed for the CCHH and CCHC variants and that involves Tyr^2, Phe^{11}, and Leu^{17} (with $Phe^{11}H\zeta,\delta,\epsilon$/$Cys^{20}H\beta$ instead of $Phe^{11}H\zeta$/$His^{20}H\delta,\epsilon$) shows that

(39) Barbato, G.; Cicero, D. O.; Bianchi, E.; Pessi, A.; Bazzo, R. *J. Biomol. NMR* **1996**, *8*, 36–48.
(40) Wüthrich, K. *NMR of Proteins and Nucleic Acids*; Wiley: New York, 1986.

Table 3. Chemical Shift Characteristics for the Folding of the Zn·CP1 Complexes[a]

		$\delta(\delta-\delta_{rc})$ / ppm				
		CP1(CCHH), pH 6.5	CP1(CCHC), pH 6.5	CP1(CCCC), pH 6.5	CP1(CCCC), pH 5.1	CP1-Δ8(CCHH), pH 6.5
Cys^4	HN	9.39 (1.08)	9.32 (1.01)	9.32 (1.01)	9.28 (0.97)	9.39 (1.08)
Ser^{10}	Hα	5.16 (0.66)	5.08 (0.58)	5.15 (0.65)	5.13 (0.63)	4.32 (−0.18)
Phe^{11}	Hζ	6.21 (−1.13)	6.16 (−1.18)	7.36 (0.02)	7.33 (−0.01)	7.14 (−0.20)
Lys^{14}	Hα	3.08 (−1.28)	3.07 (−1.29)	3.16 (−1.20)	3.25 (−1.11)	4.11 (−0.25)
Leu^{17}	HN	7.07 (−1.35)	7.02 (−1.40)	6.98 (−1.44)	7.08 (−1.34)	8.17 (−0.20)
	Hα	3.25 (−1.13)	3.17 (−1.21)	3.52 (−0.86)	3.44 (−0.94)	3.85 (−0.53)

[a] Random coil chemical shifts (δ_{rc}) were taken from ref 40.

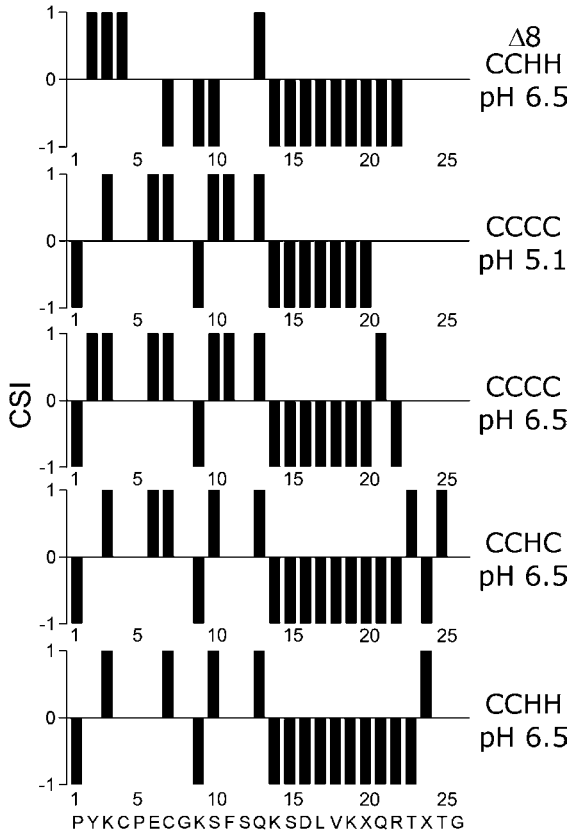

Figure 7. Chemical shift index of Hα protons for the Zn·CP1 complexes. X denotes either H or C. Four successive −1 values are indicative of a helical folding.

the hydrophobic core is packed in a similar way. When the pH is reduced to 5.1, where 76% of the complex is in the monoprotonated Zn·LH form, the NH resonances of the $V^{18}KCQRTC^{24}$ motif become even broader and most of them vanish. The chemical shifts of the other protons remain close to those of Zn·CP1(CCHH). The chemical shifts of the Zn·LH form were calculated from the data at pH 5.1 and 7.1. The CSI are the same as those measured at pH 5.1 for Zn·L (Figure S7 of Supporting Information), suggesting that Zn·LH adopts a similar $\beta\beta\alpha$ fold with a short helix from Lys^{14} to Cys^{20}. The key chemical shifts are still observed at pH 5.1 (Table 3). The main differences between pH 5.1 and pH 6.5 are observed in the C-terminal end of the peptide: the chemical shifts of Gln^{21} and Thr^{22} become closer to random coil values at pH 5.1. Together with the broadening of the NH resonances of the $V^{18}KCQRTC^{24}$ motif and the constitution of the hydrophobic core, this suggests that Cys^{24} becomes protonated when the pH is lowered.

At 298 K, the ^{1}H NMR spectrum of Zn·CP1-Δ8(CCHH) (pH 6.5) displays broad resonances, especially in the NH and

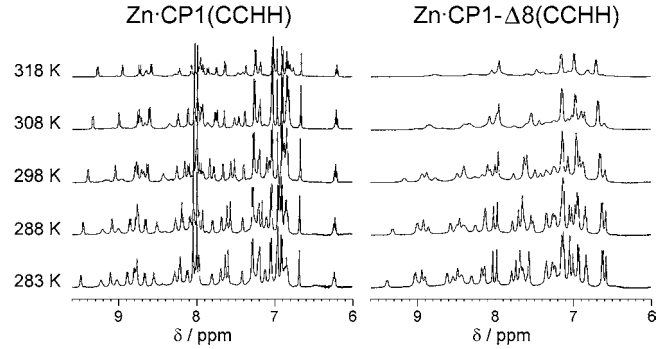

Figure 8. Amide and aromatic region of the ^{1}H NMR spectra (500 MHz, H_2O/D_2O; 9:1, v/v) of Zn·CP1(CCHH) and Zn·CP1-Δ8(CCHH) at various temperatures.

aromatic regions (Figure 8), whereas those of Zn·CP1(CCHH) are sharp, except for a few in the loop region between the β-sheet and the α-helix. All NH resonances of Zn·CP1-Δ8(CCHH) vanish at 318 K, contrary to the full-length parent peptide. When the temperature is decreased to 283 K, the NH resonances become sharp and the spectrum is well defined and spread over a wide window (6.5−9.4 ppm). This suggests that at low temperature, the peptide adopts a well-defined conformation, whereas conformational motions are favored when the temperature is raised at room temperature and above. The comparison of the spectra of Zn·CP1-Δ8(CCHH) and Zn·CP1(CCHH) at various temperatures (Figure 8) shows that the conformation stability of the latter is higher. The attribution of the ^{1}H NMR spectrum of Zn·CP1-Δ8(CCHH) was performed at 283 K and is reported in the Supporting Information. The CSI (Figure 7) reveals the helical folding of the $K^{14}SDLVKHQR^{22}$ sequence, as for the full-length complex, suggesting a similar fold for the two peptides. However, examination of the key chemical shifts listed in Table 3 highlights some differences. The resonances that are shifted upfield, due to the positioning of the H atoms in the anisotropy cone, of Tyr^2 or Phe^{11} in Zn·CP1(CCHH) adopt conventional chemical shifts values in Zn·CP1-Δ8(CCHH). None of the NOE listed above involving Phe^{11} and Tyr^2 side chains were observed. This shows that the hydrophobic core is not constituted in the heart of the structure of Zn·CP1-Δ8(CCHH). Deletion of Gly^8 in the sequence probably changes the orientation of the Phe^{11} side chain which is exposed to solvent instead of pointing toward the helix. This difference between Zn·CP1-Δ8(CCHH) and Zn·CP1(CCHH) was also confirmed by CD spectroscopy. The near-UV spectra of the two complexes as well as those of the two *apo*-peptides are displayed in Figure 9. The bands observed in this region are due to the aromatic side chains and the transitions are influenced by the

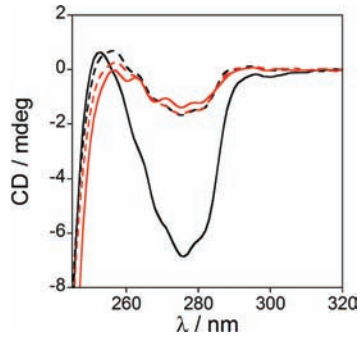

Figure 9. Near-UV CD spectra of CP1(CCHH) (black dashed line), CP1-Δ8(CCHH) (red dashed line), Zn·CP1(CCHH) (black solid line), and Zn·CP1-Δ8(CCHH) (red solid line). All samples correspond to a 3.0 mM solution of peptide in H_2O pH 7.0 at 298 K.

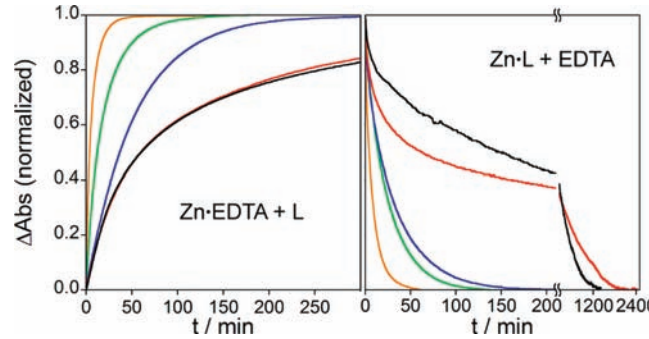

Figure 10. Normalized absorbance changes at 225 nm for competition experiments between zinc finger peptides (L) and EDTA. The plot on the left shows competitions where the peptides were added to the Zn·EDTA complex, and the plot on the right shows the competitions where EDTA was added to the Zn·L complexes. The exchange experiments were run in phosphate buffer with 30 μM peptide, zinc, and EDTA at 298 K. The kinetic traces for CP1(CCHH) (black), CP1(CCHC) (red), L_{HSP} (green), and L_{TC} (orange) were recorded at pH 6.65, and the trace for CP1(CCCC) (blue) was recorded at pH 7.35.

environment of the amino acid.[41] The intensity of the near-UV bands of Zn·CP1(CCHH) is about four times that of the *apo*-peptides, in agreement with the positioning of the aromatic amino acids in a hydrophobic core, away from water. For Zn·CP1-Δ8(CCHH), these bands are as intense as for the *apo*-peptide, suggesting that the aromatic side chains are exposed to solvent.

In conclusion, all full-length Zn·CP1 complexes adopt a $\beta\beta\alpha$ fold with a well-defined hydrophobic core. The main difference resides in the shortening of the helix as the number of cysteines increases. Concerning Zn·CP1-Δ8(CCHH), although the peptide could retain the $\beta\beta\alpha$ fold of the full-length complex, no hydrophobic core is formed by the aromatic residues and the conformation mobility of this complex is higher than that of its full-length parent.

Evaluation of the Equilibration Time for the Zinc Exchange between Peptides and EDTA. When performing the determination of the apparent binding constants, we noticed that equilibration times depended on the peptides and could reach hours. Determination of the mechanisms and kinetic rates of association and dissociation of metal to zinc finger peptides requires a careful investigation of the pH dependence of these rate constants by stopped-flow techniques.[13] Such studies are time consuming and require large quantities of peptides. Therefore, we decided to evaluate the zinc exchange kinetics from a qualitative point of view by simple metal exchange experiments between the peptide and EDTA. For each peptide, two types of experiments were performed. The first one consisted in mixing the zinc/peptide complex and 1 mol equiv of EDTA, and the second one was the reverse (Zn^{2+}/EDTA complex +1 mol equiv of *apo*-peptide). The metal exchange was followed by monitoring the change in the CysS → Zn LMCT in the UV. In order to compare the peptides, we performed these exchange experiments at pH 6.65 where all the peptides, except CP1(CCCC) (log K_{app} = 11.3), have similar log K_{app} (13.8 ± 0.3). For CP1(CCCC), the experiments were also performed at pH 7.35 where log K_{app} = 13.8.[42] The kinetic traces are displayed in Figure 10, and the half-reaction and equilibration times are summarized in Table 4. When comparing these peptides at the same binding constant (K_{app}), we notice that the equilibration times for the Cys_4 peptides are in the order of tens of minutes and increase in the order L_{TC} < L_{HSP} < CP1(CCCC). The equilibrium time increases by a factor of 2 by going from one peptide to the other in this series. The equilibrium times for CP1(CCHH) and CP1(CCHC) are even longer than that of CP1(CCCC) (about 1 day).

Table 4. Kinetics of Zinc Exchange between Zinc Finger Peptides (L) and EDTA[a]

		$t_{50}/t_{80}/t_{eq}$ (min)	
initial state	peptide	pH 6.65	pH 7.35
Zn·L + EDTA	L_{TC}	5/13/60	
	L_{HSP}	14/38/120	
	CP1(CCCC)	4/11/47	16/48/250
	CP1(CCHC)	62/690/2000[a]	
	CP1(CCHH)	147/501/1600[a]	
Zn·EDTA + L	L_{TC}	4/11/50	
	L_{HSP}	12/33/130	
	CP1(CCCC)	11/24/200	37/86/300
	CP1(CCHC)	60/239/1200[a]	
	CP1(CCHH)	60/255/1500[a]	

[a] Because of the long equilibration times for CP1(CCHC) and CP1(CCHH), it was difficult to detect the plateau indicating the end of the reaction. The error on the values given for CP1(CCHC) and CP1(CCHH) is estimated to be ±15% and ±3% for the other peptides. [a] t_{eq} corresponds to the time to reach the equilibrium, and t_{50} and t_{80} correspond to the time for 50% and 80% reaction advancement, respectively. The exchange experiments were run in phosphate buffer with 30 μM peptide, zinc, and EDTA at 298 K.

Heinz et al. reported some kinetic data for the exchange of zinc between Zn·CP1-Δ8(CCHH) and EDTA.[15] The competition was performed with excess EDTA at pH 7.0 where the apparent zinc binding constant of CP1-Δ8(CCHH) is $10^{10.6}$. In order to compare the kinetics of zinc exchange of CP1(CCHH) to those published for CP1-Δ8(CCHH), we performed a similar competition experiment by mixing Zn·CP1(CCHH) (30 μM) and EDTA (3.0 mM) at pH 5.55 where the apparent zinc binding constant of CP1(CCHH) is also $10^{10.6}$ (Figure 11). The exchange was slow with a half-exchange time of 345 s. For CP1-Δ8(CCHH), in similar conditions, the rate of zinc exchange was much faster with half-exchange time below 0.2 s.[15] This means that deletion of Gly^8 causes at least a 1700-fold increase in the rate of zinc exchange in comparison with the full-length peptide.

Discussion

Speciation and Structure of the Zn^{2+} Complexes. The speciation of the Zn^{2+} complexes of the six peptides was investi-

(41) Sreerama, N.; Woody, R. W. *Circular Dichroism of Peptides and Proteins*; Wiley: New York, 2000.

(42) At pH 6.65, the fully deprotonated form Zn·L represents 99.5%, 97%, 99.3%, 99.7%, and 99.6% of the zinc complex for CP1(CCHH), CP1(CCHC), CP1-Δ8(CCHH), L_{HSP}, and L_{TC}, respectively. At pH 7.35, 97% of the zinc complex of CP1(CCCC) is in the Zn·L form.

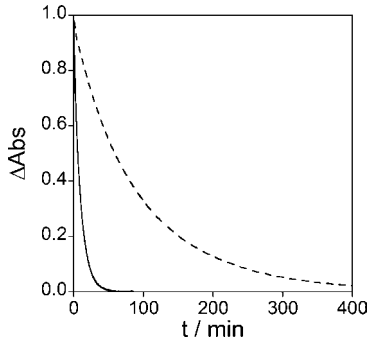

Figure 11. Normalized absorbance changes for competition experiments between 30 μM Zn·CP1(CCHH) and 0.3 (dashed line) and 3.0 mM (solid line) EDTA in Mes buffer (pH 5.55, 298 K).

gated as a function of pH. For all peptides, the predominant species at pH 7.0 is the 1:1 Zn·L complex in which all four metal binding side chains are deprotonated (thiolate for cysteine and neutral imidazole for histidine). The monoprotonated complex Zn·LH is formed only in a small amount (<1% for all peptides except CP1(CCCC) for which 5% Zn·LH is present). This corroborates the EXAFS study on CP1 peptides which is in favor of the formation of four-coordinated complexes with a fully deprotonated coordination set at pH 7.0 for all three variants of the CP1 family.[25] This is also in agreement with the studies of Mely et al.[43] and Gibney et al.[21,44] that show that Zn·L is by far the predominant species at pH 7.0 for other $(Cys)_{4-x}(His)_x$ peptides.

The NMR study of the Zn·CP1 complexes shows a similar $\beta\beta\alpha$ fold for all three full-length peptides, with a conserved hydrophobic core formed by the Tyr/Phe/Leu triad. For the CP1(CCHH) and CP1(CCHC) variants, the hydrophobic core also includes His^{20}. The structures of these three complexes differ mainly in the C-terminal region of the peptide: the length of the helix is reduced in the series CP1(CCHH) > CP1(CCHC) > CP1(CCCC). This is probably due to the shorter length of the cysteine side chain compared to histidine that forces the peptide to adopt a nonhelical conformation so that Cys^{24} binds to Zn^{2+} in the CP1(CCHC) and CP1(CCCC) variants. The pK_a for the formation of the Zn·LH complex is below 5.6 for all peptides investigated, but its value depends on the peptide. It is worth noting that the pK_a of Zn·CP1(CCCC) is ca. 1.5 pH units higher than that of the two other $ZnCys_4$ peptides $Zn{\cdot}L_{TC}$ and $Zn{\cdot}L_{HSP}$. A possible explanation resides in the structure of the site and formation of an extended hydrogen-bond network. Both $Zn{\cdot}L_{TC}$ and $Zn{\cdot}L_{HSP}$ display a well-ordered structure with seven hydrogen bonds involving the four cysteine sulfurs. It was shown that hydrogen bonds stabilize the negatively charged $Zn(Cys)_4$.[45] The C-terminal end of Zn·CP1(CCCC) appears more flexible according to the NMR data (Hα chemical shifts similar to random coil), suggesting that less hydrogen bonds are established, thereby favoring protonation of the $Zn(Cys)_4$ site. Concerning the locus of protonation in Zn·CP1(CCHH), it has been identified as the C-terminal histidine (His^{24}).[11] We did not investigate the structure of the protonated form Zn·LH for CP1(CCHC). However, due to the similarity of the K_{app} measured at the lowest pH for CP1(CCHC) and CP1(CCHH), which suggests similar species, it is likely that the protonation site is the side chain of Cys^{24}. For Zn·CP1(CCCC), since the hydrophobic core is still present at pH 5.1, Cys^{20} might remain bound to zinc and the protonation site is probably Cys^{24} also.

The impact of the deletion of a residue in the 12 amino acids spacer between the pair of cysteines and the pair of histidines was not clearly assessed on a structural point of view in the studies of Parraga et al. and Shi et al.[17,33] Parraga et al. showed that the Zn^{2+} complex of the deletion mutant of ADR1 lacking the residue just after the second cysteine in the sequence presented very broad resonances that were suggestive of more conformational motions and thus misfolding compared to the full-length parent. Shi et al. concluded that Zn·CP1-Δ8(CCHH) is at least partially folded on the basis of its 1D ^{1}H NMR spectrum in D_2O. We thus performed a more detailed structural characterization of Zn·CP1-Δ8(CCHH). This complex is indeed partially folded with the $K^{14}SDLVKHQR^{22}$ sequence in helical conformation, which suggests a fold similar to Zn·CP1(CCHH) since the CXXC motif readily forms the "zinc knuckle" structural motif when bound to zinc.[1] However, the key chemical shifts that are characteristic of the formation of the hydrophobic core in Zn·CP1(CCHH) are not observed, and the near-UV CD spectra show that Phe^{11} is exposed to solvent. Thus, the hydrophobic core is clearly lacking in the solution structure of Zn·CP1-Δ8(CCHH). This is probably the reason for the greater conformational flexibility of the deletion mutant compared to its parent, which is evidenced by the variable-temperature NMR studies (Figure 8). This deletion also has a strong impact on the binding constant and kinetics of metal exchange (vide infra).

General Considerations on Determination of the Binding Constants. The Co^{2+} and Zn^{2+} apparent binding constants of the three full-length variants of the CP1 peptide at pH 7.0 are higher than those previously reported.[24] Krizek et al. measured the apparent binding constant of Co·CP1(CCCC) from the direct UV titration of the peptide with Co^{2+}. The constant thus obtained ($10^{6.5}$) is far below the value ($10^{8.8}$) we obtained. The binding isotherm of the direct titration (Figure 2) shows that Co^{2+} binding to the CP1(CCCC) peptide is tight with a fractional saturation (the ratio between the complex concentration and the total metal concentration) near unity. Reliable binding constants cannot be obtained from direct titrations unless the fractional saturation is below 80%.[46,47] As demonstrated by Deranleau et al.,[46] the error on the binding constant increases exponentially with the fractional saturation above this limit. Therefore, the K_{app} value of $10^{6.5}$ drawn from the direct Co^{2+} titration is unreliable and indeed underestimated by 2.3 orders of magnitude. The other constants reported by Krizek et al. were derived from this constant by measurement of relative binding constants by Co^{2+} and/or Zn^{2+} titration experiments in which two peptides were mixed together. Hence, all constants reported by Krizek et al. were underestimated. Our values were obtained by competition experiments with appropriate competitors and measured on a wide pH range. The excellent agreement between the values obtained and the pH dependence expected for the binding constant is a further indication that our values are reliable. It is also noteworthy that the relative Zn^{2+} or Co^{2+} binding constants that we measured for the CP1 variants differ from those previously reported. This can arise from their underestimation of the time needed to reach the equilibrium, which is several hours for the histidine-containing peptides. For

(43) Bombarda, E.; Morellet, N.; Cherradi, H.; Spiess, B.; Bouaziz, S.; Grell, E.; Roques, B. P.; Mely, Y. *J. Mol. Biol.* **2001**, *310*, 659–672.
(44) Reddi, A. R.; Gibney, B. R. *Biochemistry* **2007**, *46*, 3745–3758.
(45) Maynard, A. T.; Covell, D. G. *J. Am. Chem. Soc.* **2001**, *123*, 1047–1058.
(46) Deranleau, D. A. *J. Am. Chem. Soc.* **1969**, *91*, 4044–4049.
(47) Deranleau, D. A. *J. Am. Chem. Soc.* **1969**, *91*, 4050–4054.

example, we determined a K_{app} for Co·CP1(CCHH) which is 50 times higher than that of Co·CP1(CCHC), whereas Krizek et al. reported a ratio of 5. The slower kinetics of Co^{2+} exchange for CP1(CCHH) compared to CP1(CCCC) (see text and Supporting Information) might be responsible for this discrepancy. In the competition titrations performed by Krizek et al., CP1(CCCC) binds to cobalt faster than CP1(CCHH), and if the system is not allowed to reach the equilibrium, the concentration of CP1(CCCC) is overestimated.

The binding constants measured for CP1(CCHH), CP1(CCHC), L_{HSP}, and L_{TC} are higher that those reported for many other zinc fingers ($K_{app} < 10^{12}$). It is worth noting that studies investigating the pH dependence of the zinc binding constant with competitors[14,21,44,48,49] systematically yield higher binding constants than studies in which the zinc affinity was determined by measuring the Co^{2+} binding constant by direct titration and then performing a titration of the Co^{2+} complex by Zn^{2+}. The titrations of $(Cys)_{4-x}(His)_x$ peptides by Co^{2+} are typically run at a peptide concentration of around 100 μM because of the low absorption coefficient of the d−d transitions ($300 < \epsilon < 1000$ M^{-1} cm^{-1}). Due to the 80% limit of the fractional saturation for accurate determination of binding constants, the limiting values for a reliable 1:1 metal/peptide binding constant at 50, 100, and 200 μM ligand concentration are $10^{5.6}$, $10^{5.3}$, and $10^{5.0}$, respectively. Therefore, any Co^{2+} binding constant above $10^{6.0}$ derived from direct titration must be considered as potentially unreliable and should be confirmed by the use of a competitor or by measuring the binding constant at a lower pH value (the variation of K_{app} can be rather well estimated by using eq 2 with pK_a values of 8.3 for cysteines and 6.5 for histidines). In addition, the limit in the fractional saturation range also applies for competition experiments where the Co^{2+} complex is titrated by Zn^{2+}. In such a titration, a $K_{app}(Zn)/K_{app}(Co)$ ratio which is too large may lead to further underestimating the zinc binding constant because of an end point that is too sharp, corresponding to an inappropriate fractional saturation. Another problem that can arise in such titrations is the interaction between the buffer and the metal ions which cannot be neglected. The use of buffer for which the Co^{2+} and Zn^{2+} affinities are not known may have a significant impact on the value of $K_{app}(Zn)/K_{app}(Co)$.[29,50] As recommended by Godwin et al., the use of BisTris buffer for such competition experiments prevents this problem. Thus, binding constants measured by direct Co^{2+} titrations followed by Co^{2+}/Zn^{2+} competitions might have been underestimated in many instances. Determination of binding constants for proteins and peptides is not straightforward, and care must be taken to correctly assess the metal−peptide affinities. Several methodological aspects of this problem have recently been reviewed.[51] We thus recommend the following steps for measurement of reliable binding constants for zinc finger peptides (or other peptides) at pH $\approx$ 7. (1) Perform a direct titration of the *apo*-peptide with the metal to check if the fractional saturation is above 80%; if not, the K_{app} can be derived from this titration; otherwise, follow steps 2−5. (2) Run a series of competition experiments in which the zinc−peptide complex ZnL is mixed with 1 mol equiv of a competitor. The use of several competing ligands with different binding strengths (EGTA, HEDTA, EDTA, TPEN, etc.) will allow a rough evaluation of the K_{app} value and the choice of an appropriate competitor, i.e., a competitor that is able to remove only a substoichiometric amount of zinc from the peptide (ideally between 0.2 and 0.8 mol equiv of zinc). The signal (CD, UV, or fluorescence) has to be recorded over an extended time span (many hours) to evaluate the equilibration time. (3) Perform the same competition by adding 1 mol equiv of *apo*-peptide to a 1:1 mixture of zinc and the competing ligand to ensure that equilibrium is reached (the same value of the signal as in 2 should be obtained; otherwise, the equilibration time may not be sufficient). (4) Perform a titration in which small amounts of the metal ion are added stepwise to a mixture of the *apo*-peptide and the appropriate competitor chosen in steps 2 and 3. The competitor can be added in excess if it removes less than 20% of zinc in steps 2 and 3. If one equivalent of competitor removes more than 80% in steps 2 and 3, use a weaker competitor (possibly in excess) to confirm the K_{app} value obtained. Be sure that equilibrium is reached before recording each spectrum. Fit as stated in the experimental section to obtain K_{app}. (5) The K_{app} thus obtained can be confirmed by performing a similar titration at a pH one unit lower or higher (another competitor may be needed or if K_{app} is low enough a direct titration might be sufficient). The consistency of the two values can be checked by ensuring that the difference in log K_{app} roughly corresponds to $n \times \Delta$pH, where n is the number of cysteines or histidines in the peptide involved in metal ion binding. Ideally, the pH dependence of K_{app} should be investigated on a wide pH range and should be fitted with eq 2 to reduce the error on K_{app} to 0.1−0.2 log units but it is time and peptide consuming as it requires also determination of the pK_a of the *apo*-peptide. However, with two measurements at different pH values, we estimate that K_{app} can be determined within 0.4 log units. This should avoid underestimating the K_{app} value by several orders of magnitude.

Zinc−Peptide Affinities. CP1(CCHH), CP1(CCHC), L_{HSP}, and L_{TC} bind zinc very tightly at physiological pH with K_{app} around 10^{15} at pH 7.0. The high values of the binding constants of the $(Cys)_4$ peptides L_{HSP} and L_{TC} match well the K_{app} values reported for three proteins, the heat-shock protein Hsp33,[52] the thioredoxin Trx2,[53] and the anaerobic RNR,[54] that contain a $Zn(Cys)_4$ site and have $K_{app} > 10^{17}$ above pH 7.5. L_{TC} mimics the structure of treble-clef zinc fingers[1,20] such as those of the GATA proteins, but its K_{app} at pH 7 ($10^{14.7}$) is higher than that of the zinc finger of the chicken GATA protein ($10^{10.3}$).[28] However, the latter constant was derived from competition experiments with CP1(CCHH). Taking into account the new values for the K_{app} of Co·CP1(CCHH), we can calculate from the data of Ghering et al. a new K_{app} value of $10^{13.7}$ for the chicken GATA finger, which is in better agreement with that of L_{TC}. All this leads to the conclusion that zinc-finger domains in proteins with well-folded structures have binding constants higher than usually believed, and we can estimate their K_{app} to be rather in the range $10^{13}-10^{16}$ at pH 7.0.

Among the six peptides investigated here, CP1(CCCC) and CP1-Δ8(CCHH) have significantly lower K_{app} than that of the four other peptides. No natural fingers having $\beta\beta\alpha$ fold and a

(48) McLendon, G.; Hull, H.; Larkin, K.; Chang, W. *J. Biol. Inorg. Chem.* **1999**, *4*, 171–174.
(49) Petros, A. K.; Reddi, A. R.; Kennedy, M. L.; Hyslop, A. G.; Gibney, B. R. *Inorg. Chem.* **2006**, *45*, 9941–9958.
(50) Magyar, J. S.; Godwin, H. A. *Anal. Biochem.* **2003**, *320*, 39–54.
(51) Xiao, Z. G.; Wedd, A. G. *Nat. Prod. Rep.* **2010**, *27*, 768–789.
(52) Jakob, U.; Eser, M.; Bardwell, J. C. A. *J. Biol. Chem.* **2000**, *275*, 38302–38310.
(53) Collet, J. F.; D'Souza, J. C.; Jakob, U.; Bardwell, J. C. A. *J. Biol. Chem.* **2003**, *278*, 45325–45332.
(54) Luttringer, F.; Mulliez, E.; Dublet, B.; Lemaire, D.; Fontecave, M. *J. Biol. Inorg. Chem.* **2009**, *14*, 923–933.

sequence similar to Zn·CP1(CCCC) are known. Such a peptide may not be suitable to sufficiently stabilize $Zn(Cys)_4$ site in comparison with other structural motifs. This is consistent with the high pK_a value (5.6) of Zn·CP1(CCCC), which shows that the binding of the fourth cysteine is less favorable than for L_{TC} or L_{HSP}. Finally, the difference in the Zn^{2+} binding constant of CP1(CCHH) and CP1-Δ8(CCHH) ($K_{Zn\cdot CP1(CCHH)}/K_{Zn\cdot CP1\text{-}\Delta8(CCHH)} = 10^{4.3}$) is striking. This highlights the huge importance of the hydrophobic core in the stability of the complex Zn·CP1(CCHH). The K_{app} of Zn·CP1-Δ8(CCHH) is $10^{10.6}$ at pH 7.0. This is close to the value of $10^{10.3}$ measured by Reddi et al. for Zn·GGG-Cys_2His_2.[21] This complex has no defined structure, suggesting that no stabilizing energy arises from the folding of Zn·CP1-Δ8(CCHH) in addition to the energy of the coordinative bonds. Therefore, we can estimate that the packing of the hydrophobic core provides a 5.7 kcal·mol^{-1} stabilizing energy to Zn·CP1(CCHH). It is interesting to note that Zn·L_{TC} shares similar K_{app} with Zn·CP1(CCHH) and Zn·CP1(CCHC), though it does not have any hydrophobic core. The extended hydrogen-bond network observed in the structure of Zn·L_{TC} and the supramolecular charge/dipole interaction that we identified between the $[Zn(Cys)_4]^{2-}$ site and the helix[20] may provide a stabilizing energy similar to that provided by the hydrophobic core.

Kinetics of Metal Exchange. We explored the kinetics of zinc exchange between EDTA and the zinc-finger peptides CP1(CCHH), CP1(CCHC), CP1(CCCC), L_{TC}, and L_{HSP} in order to compare these peptides with CP1-Δ8(CCHH).[15] The mechanism of zinc exchange is not elucidated yet. Heinz et al. argued that dissociation of zinc requires formation of a ternary complex with EDTA on the basis of the following reasoning.[15] If one assumes a direct dissociation of zinc from the peptide ($Zn\cdot L = Zn^{2+} + L$), the dissociation rate constant is given by $k_{off} = k_{on}/K_{app}$. An upper limit of k_{off} can be calculated assuming a diffusion-controlled association ($k_{on} = 10^9$ M^{-1} s^{-1}). With values of K_{app} around 10^{15} such as those measured for CP1(CCHH), L_{TC}, or L_{HSP}, this would correspond to k_{off} of 10^{-6} s^{-1} and thus minimum half-life time for zinc exchange of about 190 h, which is higher than what is observed. For this reason, Heinz et al. proposed formation of a ternary complex which accelerates zinc dissociation from the peptide. However, Bombarda et al. investigated the kinetics of zinc association to and dissociation from the HIV nucleocapsid zinc-finger peptide by stopped-flow techniques in the absence of competitors and described the mechanism of this reaction.[13] Their work establishes that direct dissociation ($Zn\cdot L = Zn^{2+} + L$) is impossible owing to the subsecond equilibration time observed that is not compatible with those expected from the k_{on} and K_{app}. The dissociation (and association also) mechanism rather involves the protonated intermediates complexes Zn·LH, Zn·LH_2, and Zn·LH_3, which show much higher dissociation rate constants than Zn·L, compatible with the fast dissociation observed. Therefore, the mechanism of zinc exchange between peptide and EDTA does not necessarily require formation of a ternary complex between Zn^{2+}, the peptide, and EDTA. However, whatever the mechanism, we observe significant differences in the exchange rates for the series of peptides. At pH 6.65, the three CCCC peptides have similar half-exchange and equilibration times, whereas those of the histidine-containing peptides are much longer. This suggests that the histidine ligands can slow down the exchange compared with cysteines. However, in these conditions all peptides do not have the same K_{app}. The K_{app} of CP1(CCCC) ($10^{11.3}$) is significantly smaller than those of the others ($\sim 10^{13.8}$). In addition, their speciations differ significantly: the monoprotonated form Zn·LH represents 0.5%, 0.5%, 12%, 2.9%, and 0.5% for L_{TC}, L_{HSP}, CP1(CCCC), CP1(CCHC), and CP1(CCHH), respectively. Bombarda et al. performed detailed kinetic studies on the association and dissociation of the NCp7 zinc finger and some of its mutants.[13,14] They demonstrated that the dissociation rate of the Zn·LH_i form increases with *i*, the number of protons bound to the zinc−peptide complex: the more protonated the complex, the faster the dissociation. The dissociation rate of the Zn·LH form is 10^3−10^5 times higher than that of the Zn·L form. We examined the metal exchange kinetics of CP1(CCCC) at a higher pH, i.e., pH 7.35, where the Zn·L form predominates (the proportion of the Zn·LH is reduced to 2.6%) and its K_{app} is similar to that of the other peptides. In these conditions (pH 7.35 for CP1(CCCC) and 6.65 for the other peptides), the half-exchange and equilibration times increase in the series $L_{TC} < L_{HSP} <$ CP1(CCCC) $\ll$ CP1(CCHC) $\approx$ CP1(CCHH). The observed differences throughout the series of peptides cannot be accounted for by a difference in K_{app} or protonation states but rather by changes in the peptides structure and amino acid composition. Indeed, we can notice that the size of the hydrophobic core in the structure of the zinc complexes increases following the order listed above for the equilibration time. The faster exchange is obtained for L_{TC}, which does not present any hydrophobic core. For the other peptides, the equilibration time increases with the number of hydrophobic amino acids packed in a hydrophobic core, L_{HSP} being intermediate between L_{TC} and CP1(CCCC) for the three CCCC peptides (Figure 1). The most striking effect is observed when we compare CP1(CCHH) and CP1-Δ8(CCHH). Deletion of a single amino acid accelerates the rate of metal exchange with EDTA by more than 3 orders of magnitude. As the two zinc complexes differ only in their folding and more precisely in the packing of the hydrophobic core, this substantiates further the role of the hydrophobic core in the control of the kinetics of metal dissociation and association. Moreover, this role has been shown also by computational methods. Li et al. studied the folding pathway of Sp1f2, a classical $\beta\beta\alpha$ Cys_2His_2 zinc finger.[55] They showed that formation of the hydrophobic core and the coordinative bonds are cooperative. They stabilize each other, and therefore, coordinative bonds cannot be broken without breaking the hydrophobic core. This suggests that the hydrophobic core in such fingers acts as a template which prevents the side chains from leaving the metal ion. It is also noteworthy that Zn·L_{TC} and Zn·L_{HSP}, which have an extended hydrogen-bond network involving the zinc-bound cysteines, are the complexes that exchange their metal faster. Therefore, hydrogen bonds may not be crucial in the kinetic control of metal exchange. Although the data presented here give only a qualitative evaluation of the metal exchange for this series of zinc finger peptides, they suggest that the presence of histidines in the coordination sphere of zinc and the presence of a well-packed hydrophobic core may play a major role in the kinetic control of metal exchange. In-depth kinetic studies similar to those performed by Bombarda et al. are however required to establish these effects on a quantitative basis. Such kinetic studies may also help in assessing the relative importance of histidines and hydrophobic cores.

Biological Relevance. The very high K_{app} of zinc fingers and the effect of histidines and hydrophobic cores on the kinetics of metal exchange may have an important biological relevance

(55) Li, W. F.; Zhang, J.; Wang, J.; Wang, W. *J. Am. Chem. Soc.* **2008**, *130*, 892–900.

for zinc-finger function and zinc homeostasis. On the one hand, zinc-finger domains of transcription factors must keep the zinc ion tightly bound to always be able to carry out DNA binding that is crucial for the cell, even in conditions of zinc depletion or high concentration of zinc binding competitors. A hydrophobic core is often encountered in the vicinity of the $Zn(Cys)_{4-x}(His)_x$ site of DNA binding domains of transcription factors. A high thermodynamic stability associated with a high kinetic stability provided by the hydrophobic core or a histidine-containing coordination set may strongly contribute to achieving this purpose. On the other hand, metallothioneins which play a buffering role for zinc in cells have to quickly acquire excess free Zn^{2+} or release Zn^{2+} in conditions of deficiency in order to maintain the zinc homeostasis.[16] It was shown that they can exchange their zinc ions with FluoZin-3 (a synthetic fluorescent zinc sensor having amino−carboxylate chelating groups as in EDTA) with half-reaction time of ~1 min.[56] Interestingly, these proteins bind zinc with cysteines only, have a very low content of hydrophobic amino acids in their sequence, and do not have any hydrophobic core in their structure. All these factors might contribute to a fast exchange of metal ions.

Conclusion

In the present work we reinvestigated the Zn^{2+} and Co^{2+} binding properties of the three CCHH, CCHC, and CCCC variants of the CP1 peptide, which is a prototype of the classical $\beta\beta\alpha$ zinc fingers, and compared them to that of a single amino acid deletion mutant of CP1 as well as to models of the treble-clef zinc fingers and of the zinc finger of the holdase Hsp33. We demonstrated that the binding strength of these two metal ions by the three full-length CP1 peptides was underestimated in previous studies by about 3 orders of magnitude. Therefore, the binding constants at physiological pH of classical zinc fingers but also other types of zinc fingers are probably higher than generally believed and can reach values in the $10^{14}-10^{15}$ range. Metal exchange experiments between the peptides and EDTA revealed a possible involvement of the presence of histidines and of a hydrophobic core in the control of the kinetics of the exchange.

Experimental Section

Abbreviations. Ac_2O, acetic anhydride; DMF, *N*,*N*-dimethylformamide; DCM, dichloromethane; DIEA, *N*,*N*-diisopropylethylamine; DTT, dithiothreitol; Et_2O, diethyl ether; Fmoc, 9-fluorenylmethyloxycarbonyl; PyBOP, (benzotriazole-1-yloxy)tris-(pyrrolidino)phosphonium hexafluorophosphate; TFA, trifluoroacetic acid; TIS, triisopropylsilane; TCEP, tris-carboxyethylphosphine; TPEN, tetrakis(2-pyridylmethyl)ethylenediamine; EDTA, ethylenediaminetetraacetic acid; HEDTA, *N*-(2-hydroxyethyl)-ethylenediamine-*N*,*N*′,*N*′-triacetic acid; EGTA, ethyleneglycol bis-(2-aminoethyl ether) tetraacetic acid; NTA, nitrilotriacetic acid; AcONa, sodium acetate; BisTris, [bis(2-hydroxyethyl)amino]tris-(hydroxymethyl)methane; DSS, sodium 3-(trimethylsilyl)-1-propanesulfonate; UV−vis, ultraviolet−visible; CD, circular dichroism.

Materials and Methods. N-α-Fmoc-protected amino acids, PyBOP, and resins were obtained from Novabiochem. Other reagents for peptide synthesis, solvents, buffers, and metal salts were purchased from Sigma-Aldrich. HPLC analyses and purifications were performed on a VWR LaPrep system. ESI-MS analyses were performed on a Thermo LXQ spectrometer. UV−vis spectra were recorded on a Perkin-Elmer Lambda 35 spectrophotometer. CD spectra were recorded on an Applied Photophysics Chirascan spectropolarimeter. UV−vis and CD spectrometers are equipped with a thermoregulated cell holder. All buffer or metal solutions were prepared with Milli-Q water (Millipore) and purged with argon. Buffer solutions were treated with Chelex 100 resin (Biorad) to remove metal traces. $Zn(ClO_4)_2$, $ZnCl_2$ (99.999%), and $CoSO_4$ (99.999%) stock solutions were prepared by dissolving the metal salt in water. Their precise concentration was determined by colorimetric EDTA titration.[57]

Synthesis of the CP1 Peptides. CP1(CCHH), CP1(CCHC), CP1(CCCC), and CP1-Δ8(CCHH) were assembled manually by solid-phase peptide synthesis on NovaPEG Rink Amide resin (substitution 0.45 mmol/g, 300 mg) using Fmoc chemistry as previously described.[20] The pseudoproline dipeptide Fmoc-Phe-Ser($\psi^{Me,Me}$pro)-OH was used to introduce the FS motif. The peptides were purified by RP-HPLC (PurospherStar RP18e 5 μm C18 particles, 50 mm × 25 mm, solvent A = H_2O/TFA 99.9:0.1, solvent B = CH_3CN/H_2O/TFA 90:10:0.1, flow rate 30 mL/min, gradient 5−70% B in 28 min). Analytical RP-HPLC (PurospherStar RP18e 5 μm C18 particles, 150 mm × 4.6 mm, gradient 5−50% B in 28 min) were performed at 1.0 mL/min with UV monitoring at 214 nm. CP1(CCHH): t_R(analytical) = 15.7 min; ESI-MS *m*/*z* = 1480.9 $[M + 2H]^{2+}$, 987.5 $[M + 3H]^{3+}$, 740.9 $[M + 4H]^{4+}$ (calcd 1480.72 $[M + 2H]^{2+}$, 987.48 $[M + 3H]^{3+}$, 740.86 $[M + 4H]^{4+}$). CP1(CCHC): t_R(analytical) = 16.4 min; ESI-MS *m*/*z* = 1464.0 $[M + 2H]^{2+}$, 976.4 $[M + 3H]^{3+}$, 732.5 $[M + 4H]^{4+}$ (calcd 1463.72 $[M + 2H]^{2+}$, 976.15 $[M + 3H]^{3+}$, 732.36 $[M + 4H]^{4+}$). CP1(CCCC): t_R(analytical) = 17.0 min; ESI-MS *m*/*z* = 2892.5 $[M + H]^{+}$, 1446.8 $[M + 2H]^{2+}$, 964.9 $[M + 3H]^{3+}$, 723.9 $[M + 4H]^{4+}$ (calcd 2892.36 $[M + H]^{+}$, 1446.68 $[M + 2H]^{2+}$, 964.79 $[M + 3H]^{3+}$, 723.84 $[M + 4H]^{4+}$). CP1-Δ8(CCHH): t_R(analytical) = 16.6 min; ESI-MS *m*/*z* = 1452.3 $[M + 2H]^{2+}$, 968.6 $[M + 3H]^{3+}$, 726.7 $[M + 4H]^{4+}$ (calcd 1452.21 $[M + 2H]^{2+}$, 968.47 $[M + 3H]^{3+}$, 726.61 $[M + 4H]^{4+}$).

NMR Spectroscopy. All of the NMR experiments were performed as already described.[20] The NMR characterizations of Zn·CP1 complexes are provided as Supporting Information.

Determination of the Proton Dissociation Constants K_{a_i} of the *apo*-Peptides. These constants were determined by ^{1}H NMR. The peptide was dissolved in D_2O (~2 mM) with TCEP (~10 mM). The sample was titrated with NaOD, and TOCSY spectra were recorded at various pH*, which corresponds to the pH measured in a D_2O solution with a pH meter calibrated in H_2O. The pK_a* values of the side chains were obtained by fitting the variations of the chemical shifts of the cysteines and their neighboring amino acids as a function of pH* with eq 3 using SPECFIT/32[36] or Kaleidagraph.

$$\delta = \left(\delta_0 + \sum_i \delta_i \times 10^{i\times pH^* - \sum_{j\le i} pK_{a_j}^*}\right) \Big/ \left(1 + \sum_i 10^{i\times pH^* - \sum_{j\le i} pK_{a_j}^*}\right) \quad (3)$$

Corrections were applied to pK_a* values to get the pK_a values corresponding to H_2O solution at 0.1 M ionic strength according to eqs 4 and 5 according to the method of Krezel and Bal.[58]

$$pK_a^*(I = 0.1) = 0.98189 \times pK_a^*(I = 0) + 0.1245 \quad (4)$$

$$pK_a(H_2O) = 0.929 \times pK_a^* + 0.42 \quad (5)$$

The details of the pK_a determination, the variations of the chemical shift against pH, and the fit to eq 3 are provided as Supporting Information for the CP1 peptides and L_{HSP}.

Each pK_a value thus obtained corresponds to the proton dissociation constant of a given histidine or cysteine side chain. The model used to fit the pH dependence of the apparent zinc binding constant requires successive macroscopic proton dissociation constants, equivalent to those measured by potentiometry. This is

(56) Krezel, A.; Maret, W. *J. Am. Chem. Soc.* **2007**, *129*, 10911–10921.
(57) Schwarzenbach, G.; Flaschka, H.; Irving, H. M. N. H. *Complexometric Titrations*, 2nd ed.; Methuen: London, 1969.
(58) Krezel, A.; Bal, W. *J. Inorg. Biochem.* **2004**, *98*, 161–166.

Table 5. pK_i Values Used To Fit the pH Dependence of K_{app} for L_{HSP} and the Four CP1 Peptides

peptide	pK_1	pK_2	pK_3	pK_4
CP1(CCHH)	6.0	6.6	7.7	8.7
CP1(CCHC)	6.3	7.5	8.3	8.9
CP1(CCCC)	7.4	8.1	8.7	9.2
CP1-Δ8(CCHH)	6.0	6.6	7.7	8.7
L_{HSP}	6.9	7.5	8.5	9.2

not the case with the pK_a values determined above, since, for example, His and Cys pK_a were determined from independent fits. The Cys and His side chain proton dissociation constants measured by NMR were converted into successive macroscopic proton dissociation constants K_i using a model accounting for noninteracting groups (eqs 6−9).[43] The pK_i values are reported in Table 5.

$$K_1 = K_{a_1}K_{a_2} + K_{a_3} + K_{a_4} \quad (6)$$

$$K_2 = (K_{a_1}K_{a_2} + K_{a_1}K_{a_3} + K_{a_1}K_{a_4} + K_{a_2}K_{a_3} + K_{a_2}K_{a_4} + K_{a_3}K_{a_4})/K_1 \quad (7)$$

$$K_3 = (K_{a_1}K_{a_2}K_{a_3} + K_{a_1}K_{a_2}K_{a_4} + K_{a_1}K_{a_3}K_{a_4} + K_{a_2}K_{a_3}K_{a_4})/K_1K_2 \quad (8)$$

$$K_4 = K_{a_1}K_{a_2}K_{a_3}K_{a_4}/K_1K_2K_3 \quad (9)$$

It is worth noting that introducing the NMR-derived pK_a values instead of the K_i values in the fit of the pH dependence of the apparent binding constants leads also to an excellent agreement between the experimental values and the fit. The impact on β_{110} and K'(ZnLH/ZnL) values is small: the highest deviations were 0.15 for log β_{110} and 0.10 for log K'.

UV−Vis and CD Titrations. The peptides were dissolved in the buffer under an argon atmosphere. The concentration of the peptide was determined by measuring cysteine-free thiol concentration using Ellman's reagent.[59] TCEP was added to the peptide solution (0.25−1.0 mM) to prevent formation of disulfide during long titrations. The binding constant of TCEP with Zn^{2+} is very weak ($\beta_{11} = 2.91$)[60] compared to those of the peptides used in this study. Thus, TCEP does not interfere with the peptide. Titrations were performed at 298 K under argon by adding aliquots of a degassed metal stock solution to a rubber-sealed quartz cell (0.4 or 1 cm path length) containing the peptide solution. UV−vis spectra were recorded every 1 nm at a scan rate of 240 nm/min. The CD signal was recorded every 1 nm with a 2 s signal averaging for each point. Each spectrum is recorded 2 times and averaged.

Determination of the Apparent Zn^{2+} Binding Constants. The apparent binding constants of the peptides with Zn^{2+} were determined at 298 K by CD titration experiments as described above but in the presence of a competitor (1−5 equiv vs peptide (∼30 μM)). The buffers used were 50 mM AcONa/100 mM KCl (pH 4.5, 5.0 and 5.5), 50 mM MES/100 mM KCl (pH 5.5 and 6.0), 50 mM Mops/100 mM KCl (pH 6.5, 7.0, and 7.5), or 100 mM phosphate (pH 6.0, 6.5, 7.0, 7.5, 8.0). The competitor (E) was chosen among TPEN, EDTA, HEDTA, and NTA. After each addition of the Zn^{2+} solution, the sample was allowed to stand for a sufficient time to reach equilibrium (up to 10 h for CP1(CCHH) and CP1(CCHC)). No oxidation was observed as judged by the CD intensity at the end of the titration when the peptide is fully loaded with zinc. The spectra were corrected for dilution. The CD signal intensity (at a fixed wavelength) against the Zn^{2+}/peptide ratio ($r = [Zn]_t/[L]_t$) was fitted to the equilibrium Zn·L + E = L + Zn·E by eqs 10−15, where S_0 and S_∞ are the CD intensities at the beginning and end of the titration, respectively, $[L]_t$ is the total concentration of peptide L, $[E]_t$ is the total concentration of competitor E, and $[Zn]_t$ is the total concentration of Zn^{2+}.

$$S = S_0 + \frac{S_\infty - S_0}{[L]_t} \times \frac{-b - \sqrt{b^2 - 4ac}}{2a}, \quad \text{for } [Zn]_t < [L]_t + [E]_t \quad (10)$$

$$S = S_\infty, \text{ for } [Zn]_t \geq [L]_t + [E]_t \quad (11)$$

$$a = K - 1 \quad (12)$$

$$b = r[L]_t - [E]_t - rK[L]_t - K[L]_t \quad (13)$$

$$c = rK[L]_t^2 \quad (14)$$

$$K = \frac{K_{ZnL}}{K_{ZnE}} = \frac{[ZnL][E]}{[ZnE][L]} \quad (15)$$

The apparent binding constants of the competitor K_{ZnE} were calculated at each pH from the published[61] pK_a and log β_{11} values for TPEN (pK_a = 2.95, 3.32, 4.85, 7.19; log β_{11} = 15.4), EDTA (pK_a = 1.51, 2.00, 2.68, 6.11, 10.17; log β_{11} = 16.4), HEDTA (pK_a = 1.60, 2.61, 5.38, 9.87; log β_{11} = 14.6), and NTA (pK_a = 0.79, 1.81, 2.48, 9.65; log β_{11} = 10.7). All protonation constants were corrected upward by 0.11 to account for 0.1 M ionic strength as recommended by Martell and Smith.[61,62] Since both the competitor and the peptide bind Zn^{2+} much more tightly than the buffer, no precipitation occurs in phosphate buffer because the concentration of free Zn^{2+} is very low. The consistency of the data obtained at a given pH with two different buffers shows that the buffers used have no influence in these competition experiments.[20]

At the lowest pH, the binding constant was determined by direct titrations in 50 mM AcONa/100 mM KCl. The titration was fit with SPECFIT/32, taking into account the binding constant of acetate with zinc.[61]

pH Titration of the Zinc Complexes. A solution (2.8 mL in a 1 cm path length cell) of peptide (∼20 μM for CP1 and 60 μM for L_{HSP}) and Zn^{2+} (1.1 molar equiv) was prepared in phosphate buffer 20 mM pH 7.0. Aliquots of HCl 1 N or HCl 0.1 N were added to vary the pH. After each addition, the pH was measured directly in the cell and a CD spectrum was recorded at 298 K. The data were fitted using SPECFIT/32.[36] The proton dissociation constants of the *apo*-peptide K_i and the β_{110} value obtained from the fit of the pH dependence of K_{app} were introduced as fixed parameters. Only the value of K'_4 and the CD spectra of ZnLH were fitted.

Determination of the Apparent Co^{2+} Binding Constants. The equilibration time for Zn^{2+} titrations of the CoCP-1 complexes was assessed by monitoring the decrease of the d−d transition after addition of 0.1 equiv of Zn^{2+} to a solution of the peptide in BisTris 100 mM/KCl 100 mM pH 7.0, containing 25 equiv of Co^{2+}. In the case of the four cysteines variant CP-1(CCCC), the equilibrium was reached after a few seconds, whereas more than 2 h was needed to equilibrate the system with the histidine-containing peptides CP-1(CCHH) and CP-1(CCHC) (see Supporting Information).

Because Co·CP1 complexes are very sensitive to traces of oxygen, in comparison with the *apo*-peptides and the Zn·CP1 complexes, long-lasting Zn/Co competition experiments were not possible. Thus, the K_{app} constants for Co·CP1(CCHH) and Co·CP1(CCHC) were derived from competition experiments with

(59) Riddles, P. W.; Blakeley, R. L.; Zerner, B. *Methods Enzymol.* **1983**, *91*, 49–60.
(60) Krezel, A.; Latajka, R.; Bujacz, G. D.; Bal, W. *Inorg. Chem.* **2003**, *42*, 1994–2003.
(61) Smith, R. M.; Martell, A. E.; Motekaitis, R. J. *Critically Selected Stability Constants of Metal Complexes Database. NIST Standard Reference Database*; National Institute of Standards and Technology: Gaithersburg, MD, 2001; Vol. 46.
(62) Martell, A. E.; Smith, R. M. *Critical Stability Constants*; Plenum Press: New York, 1974; Vol. 1.

HEDTA followed by UV−vis spectrophotometry. A solution containing the peptide (~190 μM), HEDTA (1.0 equiv), Co^{2+} (1.0 equiv), and TCEP (700 μM) in BisTris/KCl buffer was allowed to equilibrate, and the fraction of cobalt-loaded peptide was measured to derive the Co^{2+} binding constant. The fraction of *holo*-peptides (27 ± 1% and 37 ± 1% for the CP1(CCHH) and the CP1(CCHC), respectively) falls in the 20−80% range that allows accurate determination of $K_{CoCP1}/K_{CoHEDTA}$.[46,47] Competition with EGTA was also performed, but the binding to the peptide was too tight (>90% Co·CP1) to get accurate values of K_{app}, which were estimated to exceed 10^{10}, in agreement with the values obtained with HEDTA. The consistency of the value obtained for Co·CP1(CCHH) was checked by direct titrations at lower pH. Titrations were monitored by UV−vis spectrophotometry at pH 5.0 ([CP1(CCHH)] = 170 μM) and by CD at pH 5.5 ([CP1(CCHH)] = 21 μM). Measured log K_{app} values at pH 5.0 and 5.5 were 4.4 (2) and 6.0 (2), respectively. These two values and the value at pH 7.0 match well the pH dependence awaited for K_{app} (see Supporting Information). The apparent Co^{2+} binding constants of CP1(CCCC) was determined at pH 7.0 by competition experiments between Co^{2+} and Zn^{2+} monitored by UV−vis spectrophotometry at 298 K as previously described.[20] BisTris 100 mM/KCl 100 mM buffer was chosen because the binding constants of BisTris for Zn^{2+} (log β_{11} = 2.4) and Co^{2+} (log β_{11} = 1.8) are known from the literature.[29,37] This value was confirmed by a direct UV−vis titration in BisTris/KCl buffer at pH 5.9 and a competition with EGTA at pH 6.35 as described above for Co·CP1(CCHH) (see Supporting Information).

The Co^{2+} binding constant of CP1-Δ8(CCHH) was obtained by direct titration at pH 7.0 in BisTris/KCl buffer (see Supporting Information). The data were fitted with SPECFIT/32 with the Co·BisTris complex and both Co·L and Co·L_2 complexes of CP1-Δ8(CCHH). Introduction of Co·L_2 was needed to reproduce the band at 720 nm, which appears at the beginning of the titration. The spectrum of the Co·L_2 peptide was similar to that of Co·CP1(CCCC), suggesting a $Co(Cys)_4$ environment for the metal in Co·L_2.

Zinc Exchange Experiments. A solution of complex was prepared under argon by adding in the buffer (either phosphate 100 mM or Mops 50 mM/KCl 100 mM for pH 6.65 and 7.35) a solution of peptide (~700 μM in water, the precise concentration was determined by using DTNB) and a solution of $ZnCl_2$ (1.68 mM in water). A 5 μL amount of a solution of TCEP (35 mM in the buffer) was added. At t = 0, a 2.04 mM solution of EDTA was added and the absorbance at 225 nm was recorded against time. The volumes of the solutions of peptide, zinc, and EDTA were chosen so that the final concentrations were 30 μM. A second series of experiments was performed by first mixing EDTA, $ZnCl_2$, and TCEP and injecting the peptide at t = 0. No difference was observed with L_{TC}, L_{HSP}, and CP1(CCCC) peptides using phosphate or Mops as buffers, suggesting that the buffer has no influence on the rate of metal exchange. Competitions at pH 5.55 for CP1(CCHH) were performed in Mes 50 mM/KCl 100 mM buffer. The same results were obtained in AcONa 50 mM/KCl 100 mM buffer.

Acknowledgment. The authors thank Colette Lebrun for ESI-MS analysis, Manon Isaac for the synthesis of CP1(CCCC), and Nathalie Keddie for Co^{2+} titrations of CP1(CCCC). The Agence Nationale de la Recherche is acknowledged for financial support (ANR-06-JCJC-0018).

Supporting Information Available: Direct UV Co^{2+} titrations of CP1(CCHH), CP1(CCHC), and CP1-Δ8(CCHH), representative examples of titrations for determination of the apparent zinc binding constants, equations stating the pH dependence of K_{app}, details for Co^{2+}/Zn^{2+} competition experiments, a plot of K_{app} against pH for Co·CP1(CCHH), NMR characterization of the Zn·CP1 complexes, and details concerning determination of the pK_a of the *apo*-peptides. This material is available free of charge via the Internet at http://pubs.acs.org.

JA104992H